UNIVERSITY OF CALIFORNIA SAN DIEGO

Somatic Ultrastructure May Affect Calcium Signaling Dynamics in Purkinje Neurons

A thesis submitted in partial satisfaction of the requirements
for the degree of Master of Science

in

Biology

by

Lukas Paul Makrakis

Committee in charge:

Professor Brenda L. Bloodgood, Chair
Professor Padmini Rangamani
Professor Dong-Er Zhang

2021

The Thesis of Lukas Paul Makrakis is approved, and it is acceptable in quality and form for publication on microfilm and electronically.

University of California San Diego

2021

DEDICATIONS

I dedicate this thesis to my parents and brother. Without their guidance, support, and unyielding love I would not be who I am today. Thank you so much for believing in me, I love you all so much.

EPIGRAPH

"Our virtues and our failings are inseparable, like force and matter. When they separate, man is no more."

Nikola Tesla

TABLE OF CONTENTS

LIST OF FIGURES

ABBREVIATIONS

PC(s)	Purkinje cell(s)
ER	endoplasmic reticulum
PM	plasma membrane
ET	electron tomography
SBEM	serial block-face scanning electron microscopy
EM	electron microscopy
3D	three-dimensional
Climp63	cytoskeleton-linking membrane protein 63
IHC	immunohistochemistry
Ca^{2+}	calcium
IP3	inositol 1,4,5-trisphosphate
IP3R(s)	inositol 1,4,5-trisphosphate receptor(s)
PMCA(s)	plasma membrane Ca^{2+}-ATPase(s)
GPCR(s)	G protein-coupled receptor(s)
RyR(s)	ryanodine receptor(s)
CNS	central nervous system
SERCA(s)	sarco/endoplasmic reticulum Ca^{2+}-ATPase(s)
Rtn4(s)	reticulon4a(s)
IP3-Ca^{2+}	GPCR-IP3-calcium
mGluR(s)	muscarinic glutamatergic receptor(s)
CICR	calcium induced calcium release

PDE	partial differentiation equation
SOCE	store operated calcium entry
MCS	membrane contact sites
STIM1	stromal interaction molecule 1
Orai1	calcium release-activated calcium channel protein 1
TIRFM	total internal reflection fluorescence microscopy
STORM	stochastic optical reconstruction microscopy
ExM	expansion microscopy
DAPI	4′,6-diamidino-2-phenylindole

ACKNOWLEDGMENTS

I would like to express my gratitude and thanks to all of my mentors and friends in the Bloodgood, Ellisman, and Rangamani Labs who worked tirelessly to make this project possible and were a never-ending source of support, inspiration, and guidance. I am privileged to be a part of this blossoming, inclusive community that has helped me become not only a better scientist but a better person as well. To Dr. Matthias Haberl, I am so very grateful for you, as you were the one who gave me the opportunity to work on this project, and subsequently introduced me to the real world of science as an undergraduate student. I will always cherish your kind and caring mentorship, which encouraged me to continue my career in science. To Dr. Brenda Bloodgood, the head of my committee, I cannot thank you enough for your kindness and support. It was in your class that I picked myself back up, and you that encouraged me to pursue my growing love for science and research. You introduced me to this project, and for that I am eternally grateful. Thank you for your mentorship and wisdom, which has guided me throughout this process. The lessons I have learned under your wing have proved invaluable, and I expect they will continue to guide me for many years to come. To Evan Campbell, who taught me the ins and outs of the lab bench, I cannot thank you enough. From the moment I stepped into the lab, you have always been a calm, kind, and reassuring presence. I could not have asked for a better guide to navigate the dangers and wonders of laboratory science. Your constant patience has been a blessing and I am so appreciative of the many hours you spent teaching and working with me. To Ahmed Abushawish, an amazing mentor who never failed to make me laugh, thank you for guidance across the bench. To Kaitlyn Robinson and Yuning Wang, who accompanied me on this scientific journey, thank you for your friendship and camaraderie. I will cherish the memories we made through our hours spent on reconstructions, imaging, and working together, and look

forward to the new ones soon to come. Last but not least, I want to thank Dr. Padmini Rangamani and Dr. Dong-Er Zhang for being on my committee. Thank you both for your encouragement, wisdom, and faith in me. I could not have completed this without your support. Together you all have opened my eyes to the world of science and have taught me so much. I will be forever grateful for all that you have done for me.

Materials produced and used in this paper are co-authored with Haberl, Matthias G; Laughlin, Justin; Campbell, Evan P; Robinson, Kaitlyn; Wang, Yuning; Makrakis, Lukas; Nguyen, Andrew; Oshiro, Justin; Phan, Sebastien, Bushong, Eric; Deerinck, Thomas D; Ellisman, Mark H; Rangamani, Padmini; Bloodgood, Brenda L. Work from this thesis in part is currently being prepared for submission for publication of the material. Matthias Haberl is the primary investigator of this project. Lukas Makrakis is the author of this thesis and is a co-author of this material.

ABSTRACT OF THE THESIS

Somatic Ultrastructure May Affect Calcium Signaling Dynamics in Purkinje Neurons

by

Lukas Paul Makrakis

Master of Science in Biology

University of California San Diego, 2021

Professor Brenda L. Bloodgood, Chair

The organization of intracellular organelles is crucial to understanding how intracellular communication, which is shaped by signaling messengers, occurs within neurons in the brain. Neuronal communication through electrical and chemical signals causes dramatic fluctuations in calcium concentration, which regulates many neuronal processes such as synaptic plasticity, memory formation, and learning. Due to calcium's high-stakes involvement, much work has been done to understand its role, function, and regulatory mechanisms. However, it is still

unclear how the spatiotemporal dynamics of calcium are influenced by the precise orientation and positioning of the intracellular ultrastructure. While previous research has focused on the ultrastructure's influence in small spatial compartments, such as dendritic spines, its role in regulating calcium dynamics within large spatial compartments, such as the somatic space, remains unclear. In this study, we used a combination of high-resolution electron tomography (ET) and serial block-face scanning electron microscopy (SBEM) to create a precise three-dimensional (3D) reconstruction of the intracellular space of the cerebellar Purkinje soma. From these 3D reconstructions, we were able to quantify and characterize the heterogeneous nature of the endoplasmic reticulum (ER). Furthermore, we were able to quantify the cell-wide distribution patterns of integral calcium-signaling proteins using fluorescent immunohistochemistry to determine if protein populations were also heterogeneously distributed across the soma. Overall, we found that ER acts as a diffusion barrier and signal amplifier in regards to calcium/IP3 signaling. These findings demonstrate how the precise localization of membrane structures and calcium-signaling proteins influence neuronal signaling within the soma.

INTRODUCTION

The precise regulation of calcium (Ca^{2+}) signaling dynamics is required for many neuronal processes, and calcium itself is understood to be a central component of maintaining healthy neuronal function (Berridge et al., 2000; Ghosh & Greenburg, 1995). Modulated by a number of electrical and chemical signals, the spatiotemporal dynamics of intracellular calcium signaling is highly sensitive and heavily regulated (West et al., 2001; Gruol et al., 2010). If not properly regulated, this can lead to calcium overload, which may result in excitotoxicity and apoptosis (Orrenius et al., 2003). For this reason, it is not surprising that neurons have developed incredibly complex and extensive calcium signaling pathways which are made possible by a vast network of signaling proteins, calcium buffers, channels, and receptors that together regulate the spatiotemporal behavior of calcium movement within the cell (Brini et al., 2014).

Calcium regulation also shapes and modifies the morphological structure of our neurons. This has been indicated by research investigating the physiological ramifications of poor calcium handling, which resulted in abnormal cellular morphology and severely impaired motor learning ability when significantly disrupted (Sherkhane & Kapfhammer, 2013; Sugawara et al., 2013). Inositol 1,4,5-trisphosphate receptors (IP3Rs) are calcium release channels located on the membrane of the endoplasmic reticulum (ER) and are responsible for releasing the intracellular calcium stores within the ER lumen into the cytosolic space of the cell and considered to be a major regulator of intracellular calcium signaling (Berridge et al., 2000). Studies have revealed that adult mice lacking IP3R1 in Purkinje cells suffered from severe ataxia, and displayed abnormal dendritic and spine morphology, both of which continued to worsen as the mice aged (Sugawara et al., 2013). However, this is not specific to just the loss of IP3Rs, as other studies

have similarly disrupted the plasma membrane Ca^{2+}-ATPases (PMCAs), a key calcium regulator that is responsible for extruding cytosolic calcium out of the cell, which also resulted in cerebellar ataxia, and abnormal dendritic morphology (Empson et al., 2007; Kurnellas et al., 2007; Sherkhane & Kapfhammer, 2013). This exemplifies how singular points of disruption within the regulatory mechanisms of calcium handling can have profound effects on the entire cell and directly affect its structural morphology, resulting in severe physiological consequences for the organism. This is one reason why it is so crucial to understand how these regulatory molecules are localized and organized across the intracellular space, as it has serious ramifications in the cell's ability to effectively regulate calcium and thereby regulate cellular homeostasis.

Due to calcium's high-stake involvement in maintaining and regulating a number of cellular functions, such as, gene expression, secretion, and neuronal plasticity, much work has been done to understand its involved mechanisms and regulators (Berridge et al., 2000; Brini et al., 2014). Calcium is a universal second messenger and is maintained at very low concentrations during the cell's resting state (~100 nM) when compared to the extracellular environment (~2 mM) (Berridge et al., 2000; Goto & Mikoshiba, 2011). Previous research has found the plasma membrane (PM) and endoplasmic reticulum (ER) are responsible for directly modulating the concentration of cytosolic calcium by acting as a calcium source or sink (Berridge 1998). Calcium can be recruited from the extracellular space utilizing calcium channels located on the plasma membrane, or by accessing the intracellular calcium stores sequestered in the ER lumen through calcium release channels, which can be activated by a number of stimulatory agonists, such as neurotransmitters (Grienberger & Konnerth, 2012). G protein-coupled receptors (GPCRs) located on the cell surface, once activated by presynaptic neurotransmitters, cause an

internal signal transduction cascade that results in the release of other secondary messengers responsible for releasing the intracellular calcium stores of the ER (Hartmann et al., 2008; Niswender & Conn, 2010). The calcium released by the ER is capable of generating localized regions of calcium signaling, which is mediated by IP3Rs and ryanodine receptors (RyRs) located on the ER surface (Berridge 1993; Ellisman et al., 1990; Kano et al., 1995). However, the influence that the somatic ultrastructure's morphology and localization of calcium signaling molecules have on the spatiotemporal dynamics of calcium signaling remains unclear.

Much work has been done to extrapolate how neuronal morphology influences the spatial temporal dynamics of calcium in small spatial compartments, ie. dendrites and dendritic spines (Bloodgood & Sabatini, 2007; Doi et al., 2005;; Higley & Sabatini, 2008; Nimchinsky et al., 2002). Although, much is still unknown regarding how effective calcium handling is accomplished across large spatial compartments such as neuronal somas. The field has greatly benefited from previous research that developed and utilized image-based models created to quantify the spatiotemporal interplay of calcium signaling's many biological components but, these models, due to technological limitations, were unable to consider the precise intracellular morphology of the intracellular ultrastructure (Eilers et al., 1995; Fink et al., 2000). Additionally, other calcium models, with some accounting for cellular anatomical structure, still assume the calcium flux emanating from the ER to be uniformly distributed across the cytoplasmic space (Brown et al., 2008; Brown & Loew, 2012; Hernjak et al., 2005). Specifically, the two-dimensional neuroblastoma calcium wave model developed by Fink et al., 2000 varies the ER's density along the neurite to more accurately represent the results they observed using electron microscopy, in which a greater density of ER was observed in the soma when compared to the neurite. However, the model assumes that the ER is homogeneously distributed across the soma,

when in reality the ER is structurally dynamic, as it is both highly mobile and constructed of a diverse interconnected network of sheets and tubules featuring varying structural motifs (Banno & Kohno, 1998; Fink et al., 2000; Goyal & Blackstone, 2013; Nixon-Abell et al., 2016; Renvoise & Blackstone, 2010; Schroeder et al., 2019). Overall, these assumptions simplify the computational and modelling process but overlook the potential impact that the organization of intracellular features and calcium signaling proteins may have on calcium signaling dynamics. Today, it is still poorly understood how the ER's three-dimensional (3D) fine structure and positioning across the intracellular space may alter calcium signaling. Therefore, it is our intention to develop a model which incorporates realistic 3D membrane ultrastructure, along with accurate distribution patterns of calcium-signaling proteins within the somatic space, in order to investigate the influence these intracellular factors may have on calcium signaling dynamics.

In order to accomplish this, we believed testing a well-known and essential neuron was ideal for our purpose, leading us to the Purkinje neuron in the cerebellum. Purkinje cells (PCs) play an essential role within the central nervous system (CNS), being solely responsible for the synaptic output of the cerebellum, as well as facilitating long-term depression, an essential mechanism required for motor learning, which relies on a combination of sodium and calcium dynamics (Hartmann et al., 2014; Hirano, 2018). The Purkinje neuron is one of the largest singular neurons in the CNS, and because of its large soma, its detailed ultrastructure can be studied at the single cell level when utilizing high-resolution confocal and electron microscopy imaging techniques (Ellisman et al., 1990; Grienberger & Konnerth, 2012; Gruol et al., 2010; Walton et al., 1991). Using a combination of electron tomography (ET) and serial block-face scanning electron microscopy (SBEM), it is possible to more accurately and precisely define the

intracellular membrane ultrastructure, which can then be reconstructed using a neural networking deep-learning program, such as CDEEP3M, to aid in the production of these extremely intricate and expansive structures (Haberl et al., 2018). Previous research of the Purkinje cell's extensive dendritic arbor stipulates that while IP3Rs and RyRs coexist in the Purkinje cell, it is possible they may be physically separated or associated with different regions across the somatic space. (Ellisman et al., 1990; Martone et al., 1993; Sharp et al., 1999; Walton et al., 1991). Due to the soma's large intracellular space, which harbors many calcium-signaling proteins within a complex intracellular ultrastructure, it is possible we may find other heterogeneous distribution patterns or distinct spatial relationships between the somatic ultrastructure and its proteins. Overall, our present imaging and computational capabilities makes the Purkinje neuron an ideal model for studying the intracellular mechanisms that modulate calcium signaling dynamics within the cell soma.

The Purkinje soma boasts a large cytosolic volume that encompasses a highly organized intracellular space filled with organelles and populations of various proteins that regulate calcium dynamics (Fierro et al., 1998; Fierro & Llano, 1996; Gruol et al., 2010; Gruol et al., 2012). Intracellular calcium propagation is regulated by many molecules within the Purkinje cell. In particular, free-floating calcium in the soma of the Purkinje cell is heavily buffered by a number of highly expressed calcium binding proteins, called calcium buffers (Allbritton et al., 1992; Neher & Augustine, 1992). These buffers, such as calbindin, and parvalbumin, effectively dampen the flash flood of calcium in the soma, causing the free-floating calcium to act as a local rather than global messenger (Cooling et al., 2007; Allbritton et al., 1992). However, these calcium buffers do not represent the total buffering capacity within the Purkinje soma. They are assisted by other calcium pumps located on the membranes of various organelles that can also

sequester or remove calcium from the cytoplasm (Berridge et al., 2003). Located on the ER membrane, the Sarco/endoplasmic reticulum Ca^{2+}-ATPase's (SERCA's) primary function is to regulate the ER's intracellular calcium stores by reuptaking cytosolic calcium and sequestering that calcium within the ER lumen (Baba-Aissa et al., 1996; Britzolaki et al., 2018). Another calcium pump that assists in regulating intracellular calcium levels is PMCA. PMCA is highly expressed and located on the surface of the Purkinje cell's PM and extrudes excess intracellular calcium into the extracellular space in order to help maintain proper calcium homeostasis (Empson et al., 2007). Due to the great buffering capacity observed in the Purkinje cell, this suggests the soma must rely on other modes of intracellular calcium release to propagate the further depolarization of the cell. This signifies the importance of intracellular calcium stores and its modulators, most notably the endoplasmic reticulum (ER), which is regulated by a number of receptors and channels located on its surface: IP3R, RyR, and SERCA2B (Goto & Mikoshiba, 2011; Gruol et al., 2012).

The endoplasmic reticulum (ER) is a crucial intracellular organelle that plays a major role in regulating the intracellular calcium levels within all neurons (Renvoise & Blackstone, 2010). Structurally diverse, the ER is classically divided into two main subtypes of ER, ribosome-studded rough ER sheets (aka "rough" ER) and peripheral smooth ER tubules (aka "smooth" ER). It is generally understood that the two distinct morphologies are correlated with differing functional specializations and are associated with distinct ER-shaping proteins (Goyal & Blackstone, 2013). ER sheets are primarily associated with mediating biosynthesis, and modification of membrane proteins (Goyal & Blackstone, 2013). Cytoskeleton-linking membrane protein 63 (Climp63) is predominantly known for its role in generating ER sheets and has been proposed to function as a spacer that maintains ER sheet architecture (Shibata et al.,

2010). ER tubules, on the other hand, are primarily associated with lipid synthesis and delivery, as well as establishing contact sites with other organelles (Park & Blackstone, 2010; Wu et al., 2017). One of the reticulon proteins, reticulon4a (Rtn4) causes local ER curvature and is thought to induce the expansion of peripheral ER tubules (Yang & Strittmatter, 2007; Zhang & Hu, 2016). Together, the relative expression levels of Climp63 and Rtn4 are thought to determine the abundance of the two distinct ER morphologies within the cell (Shibata et al., 2010). It is understood that throughout both the soma and dendritic arbor of the Purkinje cell, a complex and continuous network of ER is present, and is essential for facilitating depolarization of the Purkinje neuron by way of receptor-specific release of the ER's internal calcium stores (Renvoise & Blackstone, 2010; Terasaki et al., 1994). One canonical calcium signaling pathway which is responsible for the signal transduction cascade that regulates the release of the ER's internal calcium stores is the GPCR-IP3-calcium (IP3-Ca^{2+}) pathway. Due to IP3-Ca^{2+} pathway's relevance regarding calcium regulation within PCs, it should provide a suitable narrative regarding our central question: How does membrane ultrastructure and protein distribution patterns influence calcium signaling dynamics in the large somatic space of the Purkinje soma? The IP3-Ca^{2+} pathway is first initiated by receptor stimulation, such as muscarinic glutamatergic receptor (mGluR) activation, which in turn causes a G-protein coupled receptor cascade to produce the second messenger, inositol 1,4,5-trisphosphate (IP3) (Goto & Mikoshiba, 2011; Berridge, 2016). Unlike free-floating calcium, which is neutralized fairly quickly by calcium buffers, IP3 has an astonishingly low degradation rate, therefore allowing it to travel across the cell, making it a 'global' agonist (Cooling et al., 2007; Allbritton et al., 1992). Once IP3 is produced, in combination with available cytosolic calcium, IP3 seeks out IP3Rs embedded into the ER and binds to it, causing a conformational change of the IP3R (Empson et al., 2012; Goto

& Mikoshiba, 2011). This results in the emptying of the ER's calcium stores into the intracellular space, further propagating the calcium wave and increasing local calcium concentration near these ER-IP3R release sites (Goto & Mikoshiba, 2011; Ross et al., 2012). This local concentration increase, surrounding the ER, triggers a third method of calcium release, known as calcium induced calcium release (CICR) (Chen-Engerer et al., 2019; Goto & Mikoshiba, 2011; Llano et al., 1994; Gruol et al., 2010). CICR is mediated by RyRs located on the ER membrane, and propagates the calcium wave further, triggering other neighboring IP3Rs and RyRs (Berridge, 2016; Goto & Mikoshiba, 2011; Chen-Engerer et al., 2019). Calcium fluxed from the intracellular stores of the ER in this manner can build upon itself, creating a regenerative calcium propagation wave as calcium is released into the cytoplasmic space (Berridge, 2016). Therefore, because calcium is subject to a specific diffusion rate, calcium signaling may be reliant on the orientation and positioning of the membrane ultrastructure within the Purkinje soma. This may also mean that the specific localization of calcium-related protein receptors located on the membrane ultrastructure could also play a substantial role in shaping calcium dynamics in large spatial compartments (Thillaiappan et al., 2017). Therefore, it is critical to investigate the interplay between the membrane ultrastructure and its calcium-signaling molecules in order to better understand how calcium regulation is mediated across the soma.

Even though much work has been done to further elucidate the mechanisms and functional consequences underlying calcium signaling dynamics, the somatic ultrastructure's role in influencing calcium regulation remains largely unknown. To further understand the role of the intracellular morphology of the soma, along with its relevant localization patterns of calcium-signaling proteins, we have developed a cell simulation model to more accurately represent calcium signaling across the somatic space. Utilizing a combination of high resolution and large-

scale volumetric electron microscopy, we were able to reconstruct a precise, 3D reconstruction of the intracellular membrane ultrastructure of the Purkinje soma. From this 3D reconstruction, we were able to characterize and quantify the spatial, radial, and structural characteristics of the ER's morphology inhabiting the somatic space. The 3D reconstruction also allowed us to analyze the orientation of the ER relative to the PM, where a large volume occupancy of ER was observed and quantified. To investigate the relative affects this close ER-PM appositioning poses on calcium signaling, a 3D partial differentiation equation (PDE) model was created to simulate calcium signaling. In order to accurately simulate the spatiotemporal dynamics of calcium signaling, the model utilizes both realistic subcellular ultrastructure and relevant calcium-signaling protein distributions. Protein distributions were obtained using fluorescence immunohistochemistry (IHC), which provided insight into the cell-wide distribution patterns of important calcium-signaling proteins across many PCs. ER-shaping proteins were also imaged and analyzed to begin to bridge the gap between our ultrastructure reconstructions and protein distribution analysis. This thesis is representative of my contributions and collaboratory work which altogether, unveils new insights into the role membrane ultrastructure plays in shaping neuronal signaling and illustrates its needed inclusion to improve calcium signaling modelling.

RESULTS

1. Somatic ultrastructure reveals non-uniform placement and orientation of major organelles in Purkinje cells

Reconstructing the intracellular space of the cerebellar Purkinje soma is complex, as multiple imaging techniques must be applied to gain relevant information on both the expansive intracellular distributions, which spans many microns, and the fine-scale structural detail of organelle features, which is found on a nm-scale. To capture the large-scale measurements across the soma, we used serial block-face scanning electron microscopy (SBEM) and reconstructed the ER and mitochondria within the somatic space of the Purkinje cell (Fig. 1.1a-c). Reconstruction of the intracellular space was accomplished by using CDEEP3M, a machine learning image segmentation program, to generate the initial segmentations of ER and mitochondria (Haberl et al., 2018). Through subsequent training of CDEEP3M and manual annotation, 3D geometric models of the intracellular organelles were reconstructed allowing us to compare their distributions within the somatic space. Precise regulation of the ER's internal calcium stores are essential for propagating intracellular calcium signaling across the soma, and for this reason we believed it appropriate to see if particular areas were void of ER. We found that ER is present in virtually every region of the soma, with a majority (93.44%) of the soma encompassing ER within a distance of 250 nm (Fig. 1.1d). However, it was found only roughly a quarter (28.03%) of the soma encompasses mitochondria within a distance of 250 nm (Fig. 1.1e). Further analysis shows that ER void areas are exclusively occupied by golgi apparatus, while mitochondria void areas are generally occupied by layered ER sheets (Haberl et al., in preparation).

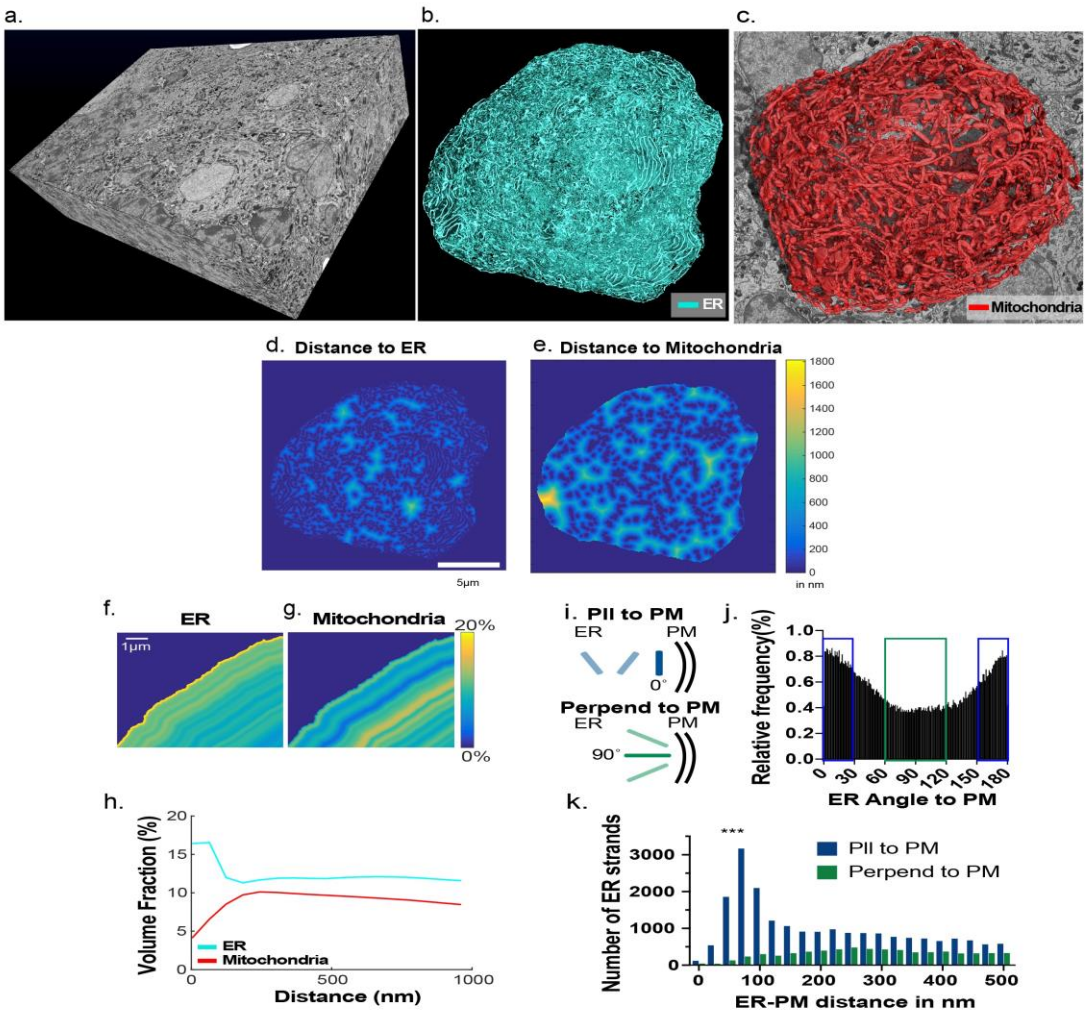

Figure 1.1 Purkinje soma ultrastructure organization analyzed by volumetric Electron Microscopy (a) A section of en-bloc stained cerebellar mouse cortex was imaged using SBEM (Serial block-face scanning electron microscopy). The ER (b) and Mitochondria (c) were computationally segmented, reconstructed, and manually corrected for final 3D model acquisition. ER (d) and Mitochondria (e) void areas are revealed with distance transformation maps, scale bar = 5µm. Color coded gradient representative of the (f) ER's and (g) Mitochondria's intracellular radial distribution based on their relative volume occupancy in relation with their distance from the PM, shown across an individual imaging plane (scale bar = 1 µm). (h) Quantification of average radial distribution of both the ER and mitochondria volume occupancy across the soma volume. (i) Parallel and perpendicular orientation of ER strands relative to the PM were defined and measured. (j-k) Orientation analysis found the ER closely apposed to the PM, within a 100 nm distance, to be preferentially oriented parallel.

Next we analyzed the intracellular radial distribution patterns of the ER and mitochondria to gain a more contextualized understanding of these major intracellular organelle's spatial distribution patterns. Radial distribution analysis was performed by collaborators by quantifying

the relative volume occupancy of the ER and mitochondria and comparing their distance from the PM (Fig. 1.1h, Haberl et al., in preparation). This informed us that a notable amount of subsurface ER resides within a 0-100nm distance from the PM (Fig. 1.1f). Conversely, a majority of mitochondria were found at a distance of 200 nm or greater away from the PM (Fig. 1.1g). This quantified analysis of organelle (ER and mitochondria) organization within the soma provides evidence that heterogeneous spatial distributions of intracellular organelles exist, which in turn may affect calcium signaling dynamics in the soma.

In order to further visualize the ultrastructure of the cerebellar Purkinje cell soma we took high-resolution electron tomography (ET) images which enabled us to capture the fine-scale detail needed to reconstruct a physiologically relevant 3D reconstruction of the somatic intracellular space (Fig. 1.2a). Using a combination of CDEEP3M and manual annotation, we were able to segment these image datasets into 5 major cellular components: ER, mitochondria, golgi apparatus, plasma membrane, and nucleus (Fig. 1.2b). Across each dataset we outlined two-dimensional reconstructions of the cellular components and then compressed multiple z-planes together to create a 3D mesh geometry that informed us of the organelle organization within the intracellular space of the Purkinje cell soma (Fig. 1.2c). Five image datasets were reconstructed in total to more accurately account for the natural spatial variance within Purkinje cells, two of which imaged the dendritic pole, and three of which imaged the axonal pole. Quantitative analysis across these 5 high-resolution ET datasets informed us of the ER's structural trends revealing it's range of diameter and length. The ER's diameter was found to have a wide range, between 10 nm and 90 nm, with an average of 39 nm (Haberl et al., in preparation). The ER's length was found to be highly variable ranging from less than 1 nm to as long as 3000 nm (Haberl et al., in preparation). Across these ET datasets, 3 structural motifs of

ER were identified using ER density maps: Layered ER sheets, ER stacks, and subsurface ER (Fig. 1.2e-f; Haberl et al., in preparation). The structural motifs identified vary in length and diameter, but more importantly seem to appear within distinct regions of the cell, supporting our hypothesis that heterogeneous spatial distribution patterns of intracellular organelles are present in the soma. Layered ER sheets preferentially orient themselves parallel and appear closely apposed to the nucleus forming large densely compact structures that surround the nucleus (Fig. 1.2e-f). ER stacks and subsurface ER represent smaller ER structural motifs that are preferentially dispersed farther from the nucleus, residing closer to the plasma membrane and form connective structures across the cytosol (Fig. 1.2e-f). Density analysis of the ER was performed across the soma and the density peaks correlated with their corresponding ER structural motifs (Haberl et al., in preparation). Across the ET reconstruction datasets, a high concentration of subsurface ER with varying orientations were recorded and quantified near the PM (Fig. 1.2d, Haberl et al., in preparation). Because the ER-PM junction represents a microdomain understood to play a fundamental role in regulating calcium signaling, we thought it important to further explore the potential role the ER's orientation, relative to the PM, may have on calcium signaling dynamics (Fig. 1.2d). Overall, across our ET volumetric reconstructions the somatic ultrastructure boasts an incredibly complex structure in which the ER is widespread, but importantly differentiated spatially by different structural motifs. Furthermore, the ER has been shown to vary greatly in size and length across the soma, and the heterogeneous distribution patterns of other organelles (mitochondria and golgi apparatus) across our 3D

reconstructions provide further evidence suggesting that the somatic space is heterogeneously distributed.

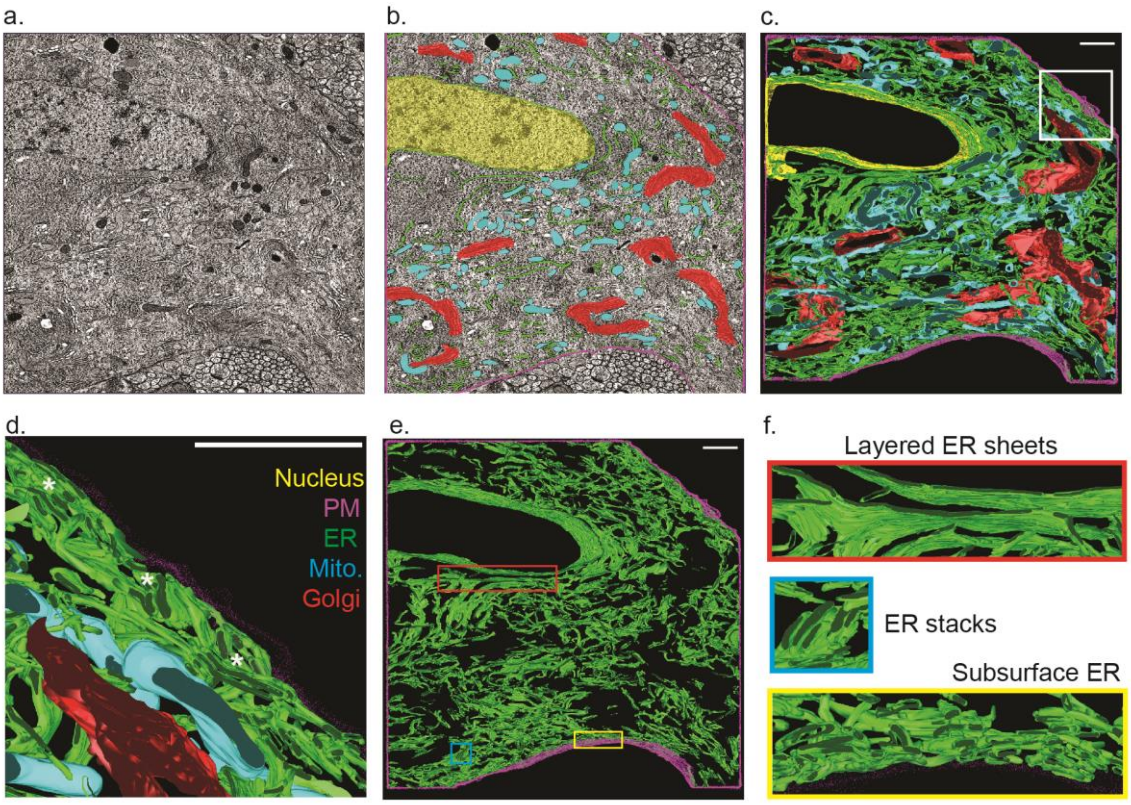

Figure 1.2 Purkinje somatic ER organization reconstructed and characterized by Electron Tomography (a) High resolution volumetric electron tomographic image datasets of the dendritic pole of the Purkinje soma were acquired. (b) Across the volumetric dataset the subcellular organelle organization was initially segmented into two-dimensional tracings, reconstructing 5 subcellular structures: nucleus (yellow), Plasma membrane (purple), ER (green), mitochondria (blue), and golgi apparatus (red). (c) 3D model view of the Purkinje soma ultrastructure reconstruction of finalized subcellular structure tracings, white box represents zoomed in portion, shown in (d); scale bar = 200 pixels. (d) Areas exemplify varying orientation of ER strands closely apposed to the PM, marked by white asterisks, and is representative of areas seen across ET datasets; scale bar = 200 pixels. (e) shows 3D model of the ER and PM reconstructions only, with colored boxes displaying ER structural subdomains seen across ET datasets. (f) Characterized ER structural subdomains: Layered ER sheets, ER stacks, and subsurface ER.

Once characterized spatially, radially, and structurally, we further characterized the ER by analyzing its orientation relative to the PM. We wished to explore the impact of the varying orientation angles these ER strands, close to the PM, may have on calcium signaling, as these ER strands are the first structures cytosolic calcium and IP3 come into contact with (Fig. 1.2d). To quantify this, parallel orientation was defined to be within 30 degrees of the horizontal (0° and

180°) relative to the PM, while perpendicular orientation was defined to be within 30 degrees of 90° (ranging from 60° to 120°) relative to the PM (Fig. 1.1i). Orientation angles outside of these ranges were not included. Across this range we found a majority of ER strands are preferentially oriented parallel near the PM (Fig. 1.1j). However, outside of parallel orientation, a great amount of variation in relative frequency data regarding orientation angles spanning from 30° to 150° suggests that the ER has no distinct orientation preference (Fig. 1.1j). Although, within a 100 nm distance of the PM it was found the ER is predominantly oriented parallel to the PM (93%), with perpendicular strands making up only a small percentage (7%) (Fig. 1.1k). This shows the preferred parallel orientation relationship is dependent on the ER's relative distance from the PM (Fig. 1.1i-k). This suggests, the orientation and spatial distribution of organelle structures have distinct distributions dependent on their localization within the soma, providing further evidence the somatic space is heterogeneously distributed.

This preferentially parallel oriented ER near the PM has the potential to impact calcium signaling. We investigated whether or not the ER acted as a diffusion barrier for either Ca^{2+} or IP3, as well as whether the close ER-PM positioning could create local concentrated microdomains of IP3 or Ca^{2+} that enhanced Ca^{2+}/IP3 signaling. A model depicting the canonical GPCR-Linked IP3R dependent calcium signaling pathway was created using idealized geometries (Haberl et al., in preparation). This model allowed us to alter the relative distance between pieces of ER, the distance between the ER and the PM, and the orientation of the ER with respect to the PM (Haberl et al., in preparation). We found, even with idealized geometries, that local concentrations of calcium released are sensitive to the ER's orientation and distance relative to the PM (Haberl et al., in preparation). Through our model, it was found a smaller ER-PM distance and parallel ER orientation led to an earlier increase in calcium concentration, when

compared to other orientation angles and ER-PM distances (Haberl et al., in preparation). Within the idealized model is a number of signaling molecules that may also have asymmetric distribution patterns that could further alter calcium signaling. Because our end goal is to create a calcium signaling model based on realistic structural and spatial geometry it is important to investigate whether the signaling molecules incorporated in the model have their own heterogeneous localization patterns across the soma.

2. Presence of Asymmetric and Symmetric distributions of calcium signaling proteins in Purkinje somas

Thus far our analysis has focused on characterizing the spatial distribution of ER structural motifs and major organelles across the soma, which we have identified in many ways to be heterogeneously distributed (Fig. 1.1 & 1.2). Currently, our model incorporates these realistic geometries and spatial distribution patterns, but up until this point has assumed a homogeneous distribution of the many signaling proteins that are incorporated into the model's GPCR-IP3-calcium signaling pathway (Haberl et al., in preparation). We sought out to analyze and quantify the localization patterns of multiple proteins: Calbindin, a calcium buffer which is robustly expressed in the Purkinje soma and binds to calcium in the cytosol; PMCA and SERCA2B, which are both Calcium-ATPase pumps that work to remove calcium from the cytosol; IP3R and RyR, which are both calcium channels embedded in the ER and are

responsible for releasing the ER's internal calcium stores; Climp63, Rtn4, and Tom20 which are associated with specific ER subdomains, and mitochondria.

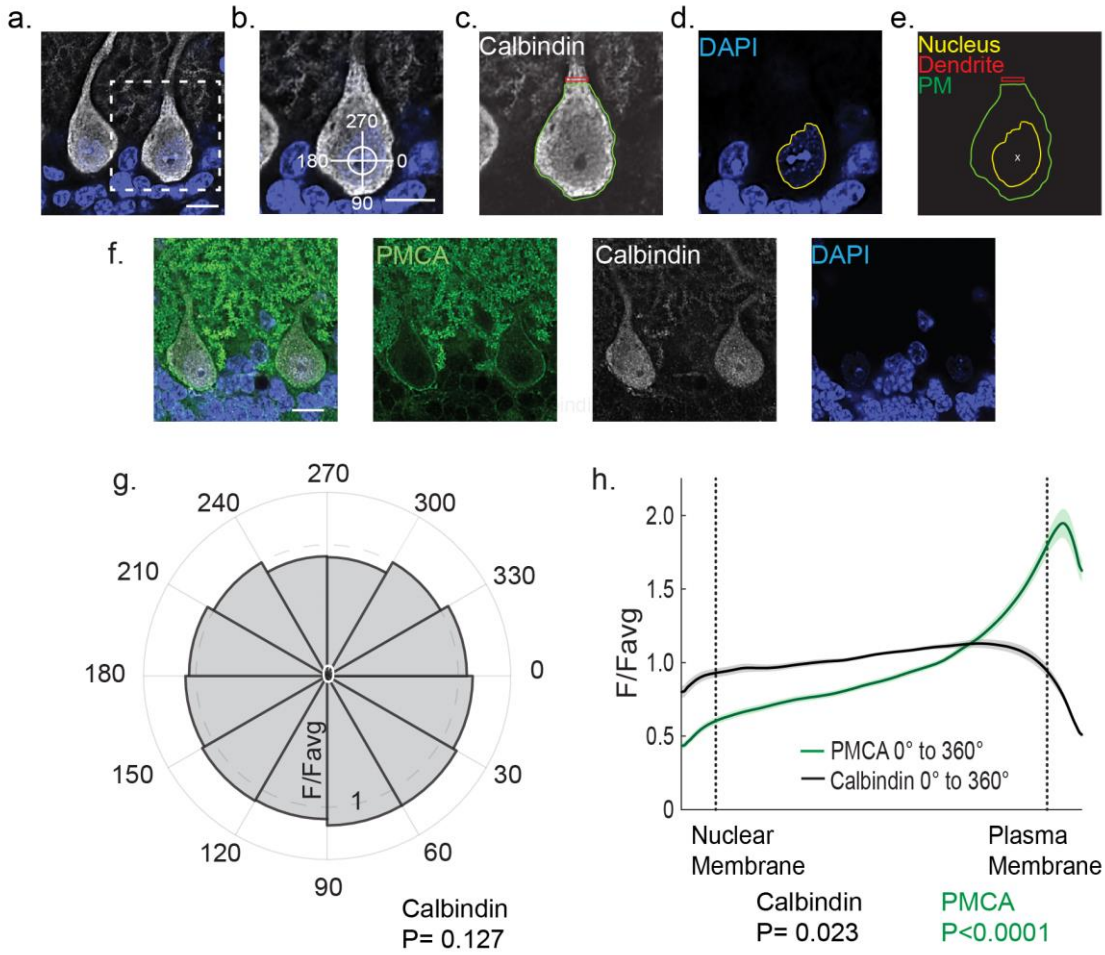

Figure 2.1 Calbindin and PMCA localization in the soma (a-e) IHC fluorescence analysis methodology (a) single cell identification for IHC fluorescence analysis. Scale bar = 10 µm. (b) Standard coordinate system, aligned linearly for each cell; creating standard cell orientation for each cell: nucleus centroid represents center (0,0), dendritic pole aligned at 270°, axonal pole aligned at 90°. Scale bar= 10µm. (c) Soma boundary mask (green) and apical dendrite mask (red) determined by Calbindin channel. (d) Nucleus boundary mask (yellow) determined by DAPI channel. (e) Composite of cell boundary masks for a single imaging plane, with x denoting the center (0,0) at the nucleus centroid. (f) Composite and single-channel fluorescent immunohistochemistry (IHC) assessment of mouse cerebellar tissue. Green channel, plasma membrane calcium ATPase (PMCA); Grey channel, Calbindin, used to visualize cell soma and dendrite; Blue channel, DAPI used to identify cell nucleus. Scale bar = 10 µm. (g) Scaled angular distribution of Calbindin divided into 12 equal 30 degree bin sections across 0° to 360°; Significance $p<.05$, n=18. Angular Fluorescence for Calbindin: p=0.127. Dotted grey lines indicate F/Favg, the normalized average fluorescence intensity, at 0.5 and 1. (h) Scaled radial distribution of average fluorescence intensity from nuclear membrane to plasma membrane across 0° to 360°; Significance $p<.05$, n=18. Radial distribution of Calbindin: p=0.023, bias towards plasma membrane. Radial distribution of PMCA: $p<0.0001$, bias toward nuclear membrane.

In order to identify cell wide localization patterns of these various calcium signaling proteins, fluorescence immunohistochemistry was performed on cerebellar mouse cortex to

identify the Purkinje soma, its nucleus, and the target protein's abundance across 18 cells for each target protein (Fig. 2.1c-e). To quantify this fluorescence data, a standard coordinate system was used for every cell and aligned linearly so that the fluorescence intensity within the soma could be analyzed along standardized angular and radial axes to measure its averaged abundance across the cell population (Fig. 2.1b).

To verify our staining protocol, we aimed to show our method could correctly identify spatial localization patterns of well documented, uniformly and asymmetrically distributed proteins within the soma. We chose calbindin, a well-documented highly expressed endogenous calcium buffer that diffuses freely across the soma's cytoplasmic space. Due to previous work, we expect it to be distributed relatively uniformly across the soma (Fierro & Llano, 1996). Protein fluorescence was captured and analyzed across angular and radial axes, as stated in methods and Figure 2.1, which qualitatively showed minimal variability in expression across the soma (Fig. 2.1a-f). Angular distribution analysis of calbindin failed to detect a significant difference ($P=0.127$), which supports that our staining and analytical methodology is sound (Fig. 2.1g). When analyzed radially, a minor but significant ($P=0.023$) bias toward the distal boundary of the cell was recorded (Fig. 2.1h). However, this biased radial distribution pattern may be the result of large bulky organelle structures, such as the mitochondria and Layered ER sheets, residing near the nucleus. These large structures may be confining and therefore limiting the cytosolic volume near the nuclear boundaries, resulting in a relative decrease of calbindin when directly compared to regions located farther from the nucleus where these structures may localize in less abundance. Evidence presented by both Climp63 (Fig. 2.2) and Tom20 (Haberl et al., in preparation), which mark Layered ER sheets and mitochondria, display a significant radial enrichment ($P<0.0001$) toward the nuclear boundaries.

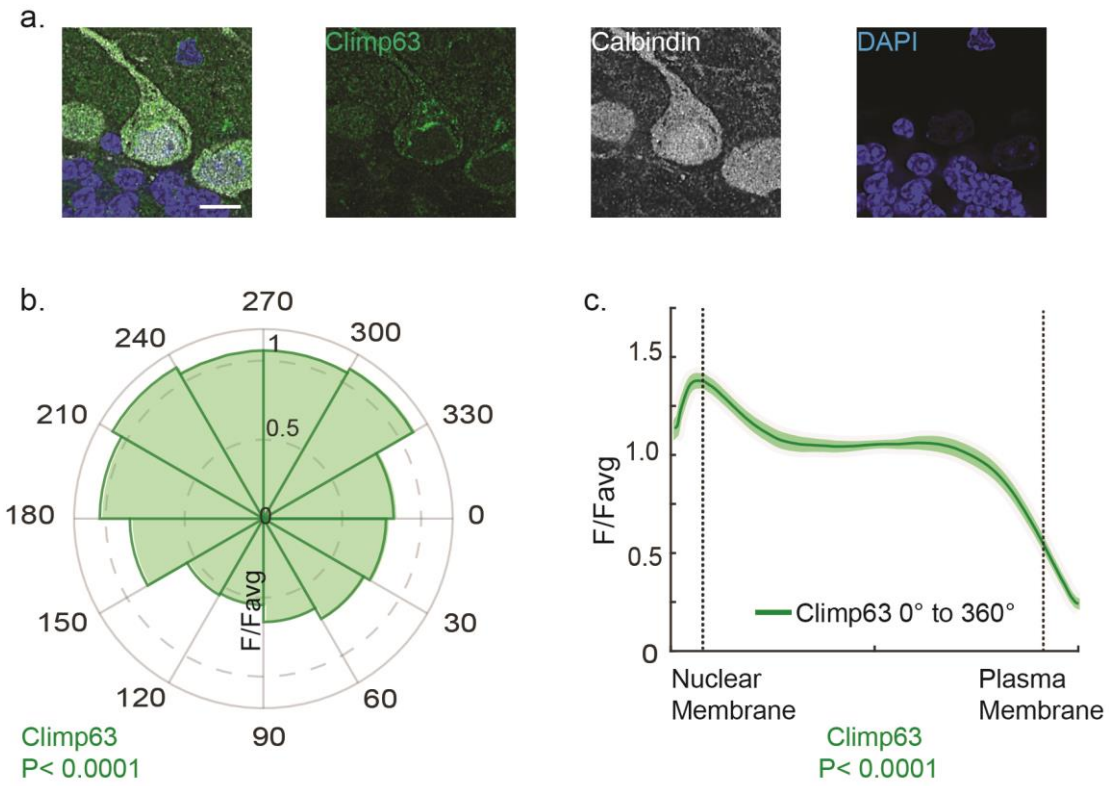

Figure 2.2 Biased Distribution of Climp63 (a) Composite and single-channel fluorescent immunohistochemistry (IHC) assessment of mouse cerebellar tissue. Green channel, cytoskeleton-linking membrane protein 63 (Climp63); Grey channel, Calbindin, used to visualize cell soma and dendrite; Blue channel, DAPI used to identify cell nucleus. Scale bar = 10 µm. (b) Scaled angular distribution of Climp63 divided into 12 equal 30 degree bin sections across 0° to 360°; Significance p<.05, n=18. Angular Fluorescence for Climp63: p<0.0001, bias toward dendritic pole. Dotted grey lines indicate F/Favg, the normalized average fluorescence intensity, at 0.5 and 1. (c) Scaled radial distribution of average fluorescence intensity from nuclear membrane to plasma membrane across 0° to 360°; Significance p<.05, n=18. Radial distribution of Climp63: p<0.0001, bias towards nuclear membrane.

While initially stained to gain a general understanding of the cell wide localization patterns of specific ER structural motifs and the mitochondria present in the soma, which were to be further explored using super-resolution microscopy techniques, their cell wide localization patterns may be useful in understanding the slight bias observed radially within our IHC calbindin dataset. Climp63, cytoskeleton-linking membrane protein 63, is predominantly known for its role in generating and maintaining ER sheets, with recent work suggesting it to function as a spacer which helps maintain ER sheet architecture (Gao et al., 2019; Shibata et al., 2010). This IHC fluorescence staining serves to provide us with a general understanding of the Layered ER sheets' distribution preferences across the soma, which we were able to characterize as large

densely compact ER structures in our ET volumetric image datasets (Fig. 2.2a; Fig. 1.2f). Climp63's angular distribution displayed a significantly high preference toward the dendritic pole region ($P<0.0001$) and radially displayed a significantly high preference toward the nuclear boundaries ($P<0.0001$) (Fig. 2.2b-c). This radial and angular enrichment of Climp63 suggests that these large ER structures localize in greater abundance near the nuclear boundaries and the dendritic pole region of the soma. Tom20, a cortical mitochondrial import receptor subunit protein, was immunostained to visualize the general distribution of mitochondria across the soma. Tom20 displays a slight angular preference on the dendritic pole ($P=0.0042$) and a significant radial bias toward the nuclear boundaries ($P<0.0001$) when analyzed across the soma, from 0°-360° (Haberl et al., in preparation). Together, Climp63 and Tom20 exemplify heterogeneously distributed organelle structural subdomains that preferentially localize in great abundance near the nuclear boundaries of the soma. These specific localization patterns of large bulky organelle structures may in fact limit the cytosolic volume available for calbindin to travel and inhabit near the nuclear boundaries, causing a relative decrease in calbindin within these areas when compared to more distal regions of the soma. This potential relative decrease in cytoplasmic space may be the reason we see a slight radial bias toward the plasma membrane within our calbindin analysis. However, this must be further explored before a definitive conclusion can be made. Overall, the calbindin fluorescence data exemplifies a largely homogeneous cell wide distribution pattern, which we expected.

Next PMCA, a ubiquitously expressed calcium-extruding enzymatic pump located on the plasma membrane, was stained to see if our methodology could accurately record and analyze well established proteins with severely polarized distribution patterns (Sepulveda et al., 2007). As suggested above, because of PMCA's known localization across the surface of the plasma

membrane, we expected PMCA to be highly polarized. Radial distribution analysis of PMCA displays an intense polarization ($P<0.0001$) confirming PMCA's distribution along the plasma membrane of the Purkinje soma (Fig. 2.1h). Together, calbindin and PMCA increase our confidence that our IHC fluorescence analysis method is able to detect both largely uniform and asymmetric fluorescence distributions within the soma. Next, we stained for proteins that modulate calcium signaling in order to quantify their cell wide distribution patterns, such as IP3R, RyR, and SERCA2B. Once quantified, these specific localization patterns will be implemented into the model which will further increase its ability to accurately depict realistic spatiotemporal calcium dynamics within the Purkinje soma, thereby increasing our confidence the model is representative of realistic biological processes.

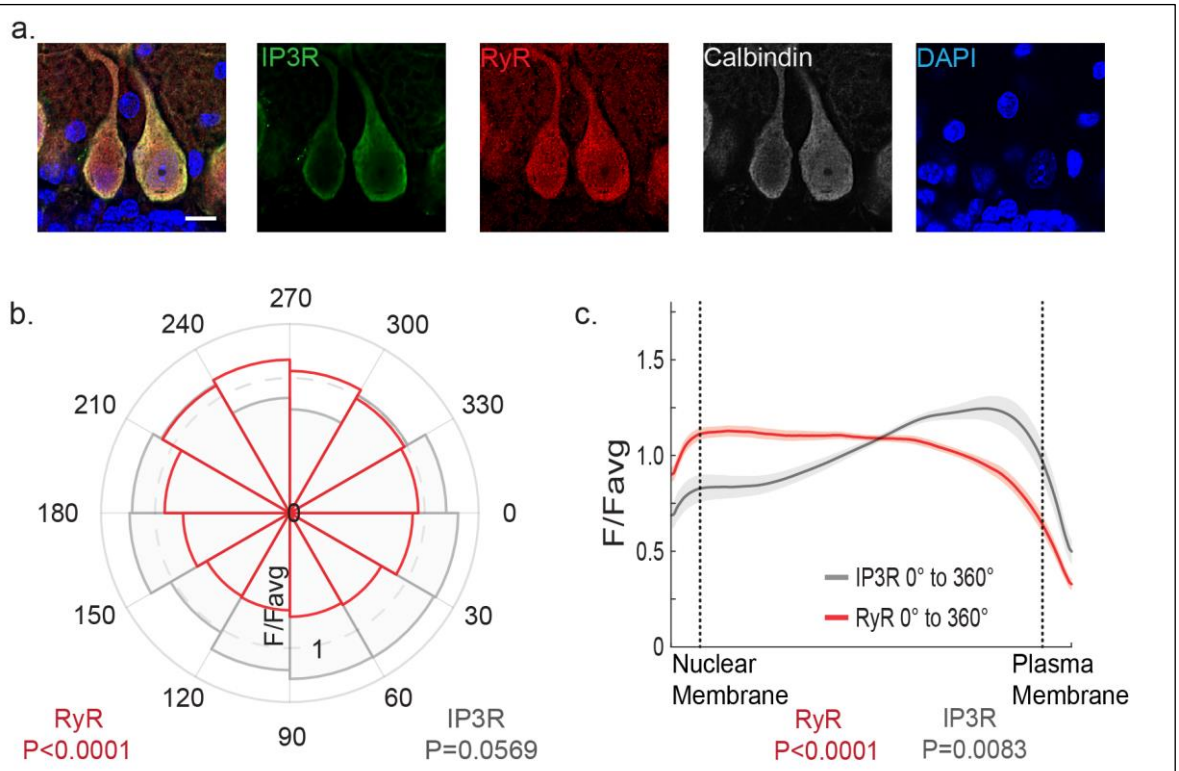

Figure 2.3 Colocalization of IP3R and RyR (a) Composite and single-channel fluorescent immunohistochemistry (IHC) assessment of mouse cerebellar tissue. Green channel, inositol triphosphate receptor (IP3R); Red channel, ryanodine receptors (RyR); Grey channel, Calbindin, used to visualize cell soma and dendrite; Blue channel, DAPI used to identify cell nucleus. Scale bar = 10 µm. (b) Scaled angular distribution of IP3R and RyR divided into 12 equal 30 degree bin sections across 0° to 360°; Significance p<.05, n=18. Angular Fluorescence for IP3R: p=0.0569. Angular Fluorescence for RyR: p<0.0001, bias towards dendritic pole. Dotted grey lines indicate F/Favg, the normalized average fluorescence intensity, at 0.5 and 1. (c) Scaled radial distribution of average fluorescence intensity from nuclear membrane to plasma membrane across 0° to 360°; Significance p<.05, n=18. Radial distribution of IP3R: p=0.0083, bias towards plasma membrane. Radial distribution of RyR: p<0.0001, bias towards nuclear membrane.

With our staining and analysis techniques established, we moved on to characterize the localization patterns of important calcium modulating proteins. Initially, we focused on IP3Rs and RyRs because both are embedded in the ER and modulate the release of the ER's internal calcium stores. This modulation of internal calcium release is essential for continued propagation of calcium across the cytoplasmic space and essential for our model, so these receptors were co-stained in order to directly compare their angular and radial fluorescence within the same cells. No significant difference in overall angular fluorescence of IP3R (P=0.0569) from 0°-360° was

detected (Fig. 2.3b). Radially, IP3R showed a significant radial bias (P=0.0083) toward the distal boundaries of the soma from 0°-360° (Fig. 2.3c). However, when analyzing individual degree bins it should be noted that degree bins 240°-270° and 270°-300° showed IP3R to be significantly less abundant within these regions of the dendritic pole (Fig. 2.3b). In congruence with IP3R's high abundance within the axonal pole regions and the significant radial trend signifying increased abundance near the PM, it is possible IP3Rs may be more highly associated with subsurface ER closely apposed to the PM. This could potentially explain why there is a significant decrease in IP3R abundance at the 270° region, because this is where the dendritic opening is present. Essentially, this is the only region lacking PM, which subsequently may be causing a reduction in overall abundance of subsurface ER within the 270° region (Fig. 2.3). Conversely, RyR was found to have a significantly polarized angular distribution ($P<0.0001$) bias, favoring the dendritic pole regions (Fig. 2.3b). Our radial analysis of RyR also indicates a strong fluorescence enrichment toward the nuclear boundaries of the cell resulting in a significantly biased proximal distribution ($P<0.0001$) preference for RyRs (Fig 2.3c). The relevant decrease in abundance of RyRs on the axonal pole, in congruence with its proximal radial bias, suggests the possibility that RyRs may be more highly associated with more proximally localized ER. Importantly, IP3R's and RyR's distinct angular and radial localization patterns support our hypothesis that calcium signaling proteins can be heterogeneously distributed in the Purkinje soma.

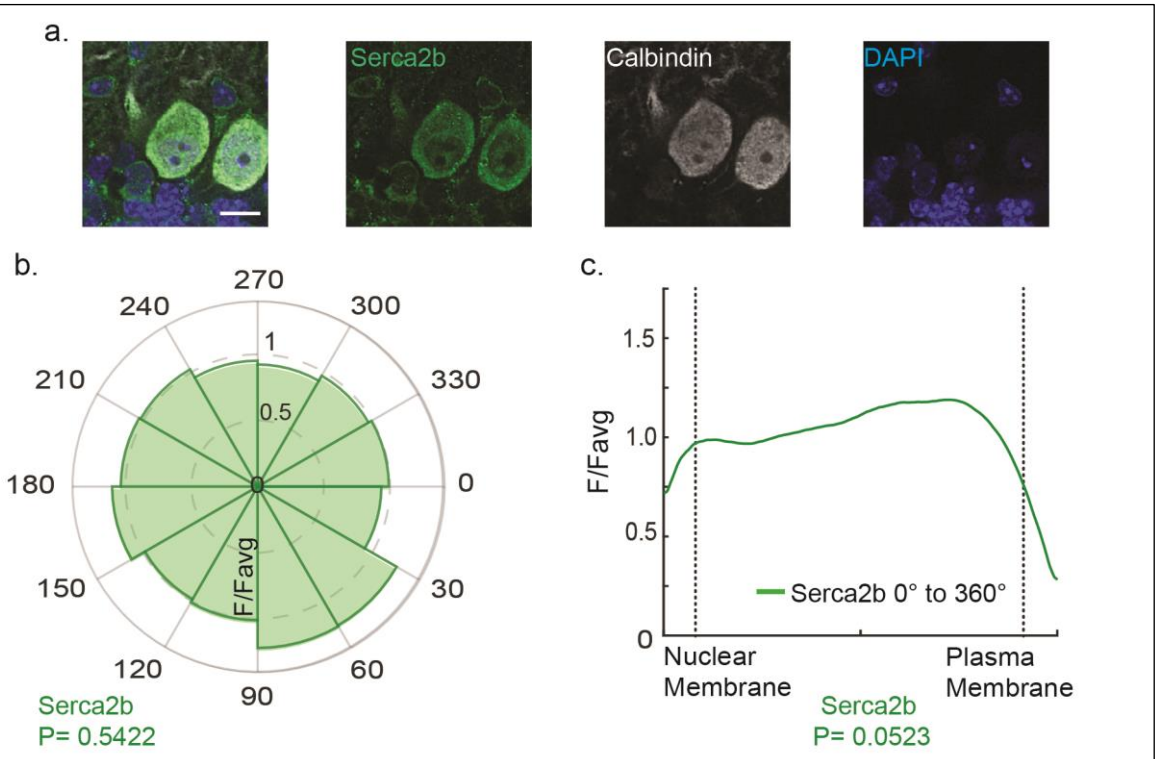

Figure 2.4 Localization of SERCA2B (a) Composite and single-channel fluorescent immunohistochemistry (IHC) assessment of mouse cerebellar tissue. Green channel, sarco-endoplasmic reticulum calcium ATPase (SERCA2B); Grey channel, Calbindin, used to visualize cell soma and dendrite; Blue channel, DAPI used to identify cell nucleus. Scale bar = 10 µm. (b) Scaled angular distribution of Serca2B divided into 12 equal 30 degree bin sections across 0° to 360°; Significance p<.05, n=18. Angular Fluorescence for SERCA2B: p=0.5422, bias toward dendritic pole. Dotted grey lines indicate F/Favg, the normalized average fluorescence intensity, at 0.5 and 1. (c) Scaled radial distribution of average fluorescence intensity from nuclear membrane to plasma membrane across 0° to 360°; Significance p<.05, n=18. Radial distribution of SERCA2B: p=0.0523.

SERCA2B is another important calcium modulating protein we stained. Its primary function is monitoring and regulating the ER's internal calcium stores by transporting cytosolic calcium back into the ER once these calcium stores are depleted. SERCA2B, formally known as sarco/endoplasmic reticulum calcium ATPase pump, is located on the ER membrane and is an integral regulator in maintaining the ER's internal calcium stores. Just as IP3R and RyR represent integral calcium release channels that perpetuate regenerative calcium propagation across the cytoplasmic space, SERCA2B aids the buffering capacity of the soma which helps maintain proper calcium homeostasis, as well as regulate the ER's internal calcium

concentration. We found SERCA2b to be uniformly distributed across the soma, displaying no significant difference in either its angular (P=.5422) or radial (P=.0523) distribution (Fig. 2.4b-c). While we don't see a statically significant effect, it's worth noting that there is a substantial trend seen radially moving toward a potential increase closer toward the nuclear membrane, and this data set has a smaller n-value than other datasets, with five cells being represented rather than eighteen. Therefore, it is possible that given a higher n-value, we would detect a radially heterogeneous distribution. Overall, SERCA2B was not found to be heterogeneously distributed and until more data is acquired our model’s assumption assuming a homogeneous distribution of SERCA2B does not need to be corrected.

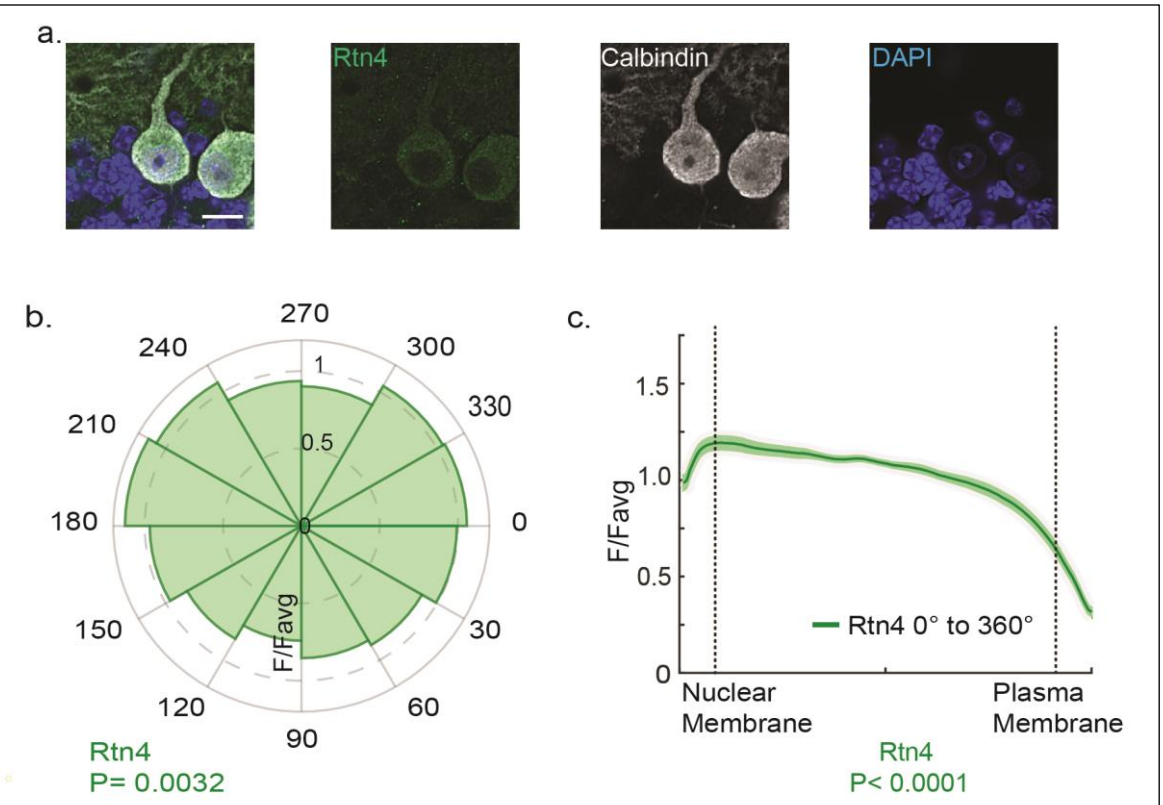

Figure 2.5 Biased Distribution of Rtn4 (a) Composite and single-channel fluorescent immunohistochemistry (IHC) assessment of mouse cerebellar tissue. Green channel, reticulon 4 (Rtn4); Grey channel, Calbindin, used to visualize cell soma and dendrite; Blue channel, DAPI used to identify cell nucleus. Scale bar = 10 µm. (b) Scaled angular distribution of Climp63 divided into 12 equal 30 degree bin sections across 0° to 360°; Significance p<.05, n=18. Angular Fluorescence for Rtn4: p=0.0032, bias toward dendritic pole. Dotted grey lines indicate F/Favg, the normalized average fluorescence intensity, at 0.5 and 1. (c) Scaled radial distribution of average fluorescence intensity from nuclear membrane to plasma membrane across 0° to 360°; Significance p<.05, n=18. Radial distribution of Rtn4: p<0.0001, bias towards nuclear membrane.

Rtn4, reticulon4a, was also immunostained for and is understood to promote ER tubule formation and cause local ER curvature (Gao et al., 2019; Goyal & Blackstone, 2013). Importantly, Rtn4 is believed to be excluded from “sheet-like ER structures" and recently has been identified to be present in highly dynamic peripheral ER matices, that are made up of dense layers of ER tubular structures (Nixon-Abell et al., 2016). Recent work has suggested these dense layered ER tubular structures have been misidentified previously by standard confocal imaging techniques that lack the spatiotemporal resolution to distinguish between uniform layered ER sheets located near the nucleus, where the cell is widest, and peripheral ER matrices

localized in more distal regions of the cell, where the cell is much thinner. This initial Rtn4 immunostaining was done in order to compare its results with Climp63 and co-stained super-resolution microscopy experiments were planned to gain greater insight in the spatial distribution of these specific ER structures. We found Rtn4 has a slight angular preference toward the dendritic pole ($P=0.0032$) when analyzed from 0-360 degrees (Fig. 2.5b). Radially, Rtn4, like Climp63, is significantly polarized ($P<0.0001$) near the nuclear boundaries, signifying a high enrichment near the nucleus (Fig. 2.5c). While we understand our resolution is not high enough to distinguish between these structures presently, the potential conflation observed between Climp63 and Rtn4 exemplifies the complex nature of the ER's fine ultrastructure present within the Purkinje soma. Future directions to be explored include using a combination of super-resolution microscopy techniques in order to more solidly distinguish the differences between these structures' specific spatial localization patterns within the soma of the Purkinje cell.

IHC protein distribution analysis was done initially to gain insight into the general cell-wide distribution patterns of important calcium modulating proteins. IP3R and RyR were found to be heterogeneously distributed across the soma, while SERCA2B was found to be largely homogeneously distributed. Even though more work must be done utilizing super-resolution microscopy techniques in order to more faithfully populate the final model, parameter sweeps varying relative densities of IP3R and RyR present on the ER membrane were performed utilizing the idealized geometry model discussed previously (Haberl et al., in preparation). It was found these varying receptor densities had a major impact on the amount of total calcium molecules released, providing evidence that heterogeneous protein distributions may significantly influence calcium signaling dynamics within the somatic space (Haberl et al., in preparation).

DISCUSSION

Understanding calcium signaling dynamics has been and continues to be an important and evolving field in neuroscience. This research and its findings have expanded our understanding by providing evidence that the orientation of heterogeneous membrane ultrastructure and the distribution of calcium signaling molecules shape the spatiotemporal dynamics of calcium in the soma. By using a combination of SBEM and high-resolution ET, we were able to reconstruct and characterize the membrane ultrastructure of the Purkinje cell soma (Fig. 1.1-1.2, Haberl et al., in preparation). The ER has been shown to be an extensively widespread and morphologically heterogeneous intracellular organelle that plays an important role in maintaining proper regulation of calcium dynamics (Renvoise & Blackstone, 2010; Voeltz et al., 2002). Through our 3D reconstructions, we confirmed the ER to be a continuous and intricate interconnected network featuring various structural motifs that were spatially differentiated across the soma, filling the cytoplasmic space between the nucleus and plasma membrane (Fig. 1.1-1.2, Haber et al., in preparation). Further analysis of the ER revealed a high volume of subsurface ER to be preferentially oriented parallel and closely apposed to the PM (Fig. 1.1-1.2, Haberl et al., in preparation). This data corroborates with other studies that have documented a high percentage of ER-PM contact sites in neuronal cell bodies made by ER cisternae, in which the ER covered a much larger fraction of the PM comparatively to smaller neuronal compartments, such as dendrites, axons, and spines (Wu et al., 2017). The great abundance of ER closely apposed to the PM seen in the soma may be indicative of the functional importance ER has in maintaining proper calcium signaling dynamics across large spatial compartments. Functionally, this highly abundant and parallel oriented subsurface ER near the PM may impact calcium signaling dynamics as a physical barrier, as well as be associated with

store operated calcium entry (SOCE) (Chang et al., 2017; Subedi et al., 2017; Wu et al., 2017). To test how the varying orientation angles and positioning of the ER relative to the PM affect calcium signaling dynamics, a model utilizing idealized geometry was constructed (Haberl et al., in preparation). The model tests a variety of parameters giving us the ability to vary ER-PM distance, and ER orientation relative to the PM (Haberl et al., in preparation). It was found that parallel orientation resulted in the earliest increase in local calcium concentration, at 120 ms, suggesting parallel orientation may be favored in order to generate local microdomains of concentrated calcium more quickly near the PM (Haberl et al., in preparation). It was also found that larger amounts of calcium molecules were released overall when the distance between the ER-PM was the smallest, and the ER orientation to the PM was parallel or closest to parallel (Haberl et al., in preparation). This suggests local microdomains of calcium are sensitive to the ER's relevant position, orientation, and apposition to the PM. This provides evidence that the somatic ultrastructure's heterogeneous morphology may influence calcium signaling dynamics across the Purkinje soma.

A potential reason for the great abundance of parallel oriented ER near the PM within the Purkinje soma could be a functional need which requires many ER-PM membrane contact sites (MCS). ER-PM MCS have been found to mediate SOCE through the interaction of STIM1 (stromal interaction molecule 1) located on the ER and Orai1 (calcium release-activated calcium channel protein 1) located on the PM, which function to replenish internal ER calcium stores, once the calcium stores are depleted (Chang et al., 2017; Chung et al., 2017; Stefan et al., 2013). Recent studies have suggested SOCE (via STIM1-Orai proteins interaction) is required for refilling ER calcium stores in non-firing Purkinje cells held at resting membrane potential, however SOCE's role in refilling depolarization-evoked calcium depletion seems to be minimal

and more work must be done to fully understand it in its entirety (Hartmann et al., 2014; Kraft, 2015). The same study also showed mGlur1-dependent synaptic signaling, in which the GPCR-IP3-calcium pathway is reliant on to occur, to be completely halted in the absence of STIM1, suggesting STIM1 may be a key regulator of calcium signaling (Hartmann et al., 2014). This suggests Purkinje neurons may depend on SOCE as a mechanism for maintaining calcium homeostasis and therefore may depend on the somatic ultrastructure mediating ER-PM MCS in order to maintain the ER's internal calcium stores. Future developments of the model may wish to further explore the functional ramifications of SOCE on calcium signaling dynamics in Purkinje somas, in order to implement SOCE to continue to increase the model's physiological relevance.

Once we found evidence the somatic ultrastructure was heterogeneously distributed, we sought to determine if calcium signaling molecules were also heterogeneously distributed across the somatic space. Fluorescence IHC staining and confocal microscopy was performed in order to gain a first pass understanding of cell-wide distribution patterns of proteins involved with the IP3-Ca^{2+} pathway. We were able to validate our protein distribution staining and analytical methodology by detecting both highly polarized and widely distributed proteins. PMCA is a calcium extruding pump, previously described as an integral regulator responsible for maintaining intracellular calcium levels and is highly expressed on the plasma membrane of Purkinje cells which is important for maintaining intracellular calcium levels (Empson et al., 2007; Sherkhane & Kapfhammer, 2013). PMCA's significant radial bias toward the PM confirms this and indicates we are able to accurately detect heterogeneous distribution patterns (Fig. 2.1). Calbindin, a well-known highly expressed and endogenous calcium buffer, was expected to be relatively homogeneously distributed across the soma (Fierro & Llano, 1996;

Maskey et al., 2010). Our experiments confirmed this previously held assumption as no significant difference in calbindin's angular distribution was detected, indicating it to be relatively widely and evenly distributed across the somatic space (Fig. 2.1). This being said, radial analysis indicated a slight but nonetheless significant bias toward the distal boundaries of the cell (Fig. 2.1). However, a possible biological explanation for this radial bias may be the result of large bulky organelle structures, such as mitochondria and Layered ER sheets, residing near the nucleus. These large structures may be confining and therefore limiting the cytosolic volume near the nuclear boundaries, resulting in a relative decrease of calbindin when averaged and directly compared to areas near the plasma membrane. This explanation is supported by our IHC staining of Climp63 and Tom20, which both display significantly high radial enrichment near the nuclear boundaries, as well as significant angular biases, favoring the dendritic pole (Fig. 2.4, Haberl et al., in preparation). In addition, analysis across the EM ultrastructure reconstruction indicates a high density of Layered ER sheets surrounding the nucleus (Fig. 1.2; Haberl et al., in preparation). Furthermore, radial analysis across the SBEM dataset found a majority of mitochondria to be positioned 200 nm or farther from the PM, occupying areas closer to the nucleus (Fig. 1.1; Haberl et al., in preparation). Together, these findings indicate large bulky organelle structures, marked by Climp63 and Tom20, to be heavily localized within the perinuclear region of the somatic space. It should be noted that while no significant difference was detected angularly, calbindin expression was reduced in the dendritic pole region when compared to the axonal pole region with degree bins 240°-300° resulting in the greatest overall decrease (Fig. 2.1g). This antiparallel relationship, displayed between calbindin, and both Tom20 and Climp63 suggests the increased presence of these large organelle structures may limit cytosolic volume near the nucleus, which may be why a slight radial bias toward the plasma

membrane is observed for calbindin. Overall, calbindin and PMCA indicate our ability to detect both highly polarized and widely distributed proteins, in the somatic space.

In order to populate our model faithfully, a precise understanding of the cell wide distribution patterns is needed for all of the calcium signaling proteins in the GPCR-IP3-calcium pathway. Unlike PMCA and calbindin, other calcium signaling protein's distribution patterns are not nearly as well understood in the Purkinje soma. IP3R, RyR, and SERCA2B are of particular interest as they all reside on the ER membrane and regulate the release and replenishment of the ER's internal calcium stores. A previous two-dimensional model depicting calcium dynamics in neurites of neuroblastoma cells similarly believed it essential to analyze the distribution of critical proteins that may alter calcium dynamics dependent on their localization patterns across the neurite (Fink et al., 2000). Our IHC analysis indicates IP3R and RyR to be heterogeneously distributed across the soma, while SERCA2B was found to be largely homogeneously distributed (Fig. 2.3; Fig. 2.4). IP3R fluorescence was found to be significantly enriched near the PM, indicating a heterogeneous radial distribution pattern (Fig. 2.3). This finding corroborates with a recent study that used a combination of TIRFM (total internal reflection fluorescence microscopy) and STORM (stochastic optical reconstruction microscopy) to image live cells in high resolution and discerned through their experimentation that IP3R calcium mediated puffs were localized near the PM and caused predominantly by immobile IP3R clusters (Thillaiappan et al., 2017). Therefore, in combination with our own findings, it is possible that immobile IP3R clusters near the PM may be more heavily localized along the subsurface ER near the PM relative to ER in other regions of the soma. It is therefore pertinent to further investigate IP3R's distribution along the subsurface ER near the PM using super-resolution imaging techniques, such as expansion microscopy (ExM), to determine if significant variations of IP3R density exist

across the somatic space as this may directly alter calcium signaling dynamics (Tillberg et al., 2016).

RyR, like IP3R, was also found to be heterogeneously distributed. According to our IHC analysis, RyR is both angularly and radially polarized featuring a significant enrichment toward the nuclear boundaries and the dendritic pole (Fig. 2.3). RyRs are activated when an increased concentration of cytosolic calcium is sensed, resulting in CICR, a process which amplifies the regenerative calcium wave across the cytoplasmic space (Gruol et al., 2010; Llano et al., 1994). Together, a number of past studies indicate the important functional role RyR may have in influencing calcium signaling in Purkinje cells and was found to significantly amplify large calcium signals (Gruol et al., 2010; Kuwajima et al., 1992; Llano et al., 1994). It was also found that the perinuclear calcium signals were larger than the calcium signals recorded near the PM, indicating calcium signals are amplified as calcium transverses the somatic space (Gruol et al., 2010). From these observations, they concluded this enhanced amplification was likely the result of CICR mediated by RyR (Gruol et al., 2010). If correct, this is potential evidence suggesting RyR may be more heavily associated with ER situated near the nucleus, which our IHC analysis supports, but more data must be collected before any definitive conclusions can be made. Unlike RyR and IP3R, SERCA2B was found to be largely homogeneously distributed across the soma (Fig. 2.4). Previous studies have indicated that across neuronal cell types, SERCA2b expression is highest in Purkinje neurons, with the soma boasting the greatest expression levels (Baba-Aissa et al., 1996; Sepulveda et al., 2004). This is in agreement with our own observations, so at this time the uniform distribution assumption made within our model does not need to be altered in regards to SERCA2B (Fig. 2.4; Haberl et al., in preparation).

While not directly a part of the GPCR-IP3-calcium pathway, Climp63, Rtn4, and Tom20 highlight structural subdomains across the somatic ultrastructure which will allow us to compare our protein distribution analysis more directly with our 3D ultrastructure reconstructions. By utilizing a number of super-resolution imaging techniques, we will be able to further characterize the morphology of the intracellular space and assess the localization of Climp63, Rtn4, and Tom20 with greater spatial resolution (Gambarotto et al., 2019; Nixon-Abell et al., 2016). These experiments will help to confirm our findings, regarding the complex, dynamic, and heterogeneous ultrastructure which we observed and reconstructed within our experiments. Other future directions, to continue to better the model, include further exploring localization patterns of relevant calcium signaling proteins utilizing super-resolution microscopy techniques (Gambarotto et al., 2019; Wassie et al., 2019). Recent studies have identified new applications utilizing variations of ExM, in which proteins are anchored to the ExM gel and then expanded, resulting in enhanced spatial resolution while maintaining protein retention (~4.5x) (Tillberg et al., 2016; Wassie et al., 2019). Utilizing these techniques will allow us to observe and quantify spatial distributions of key calcium signaling molecules in subcellular domains across the soma with enhanced spatial resolution. Co-localization staining between varying combinations of calcium signaling proteins may provide insight in how their localization relative to one another could impact their functional role within ER nanodomains (Biwer & Isakson, 2017; Thillaiappan et al., 2017; Wu et al., 2017). In addition to our IHC analysis, these combined results will provide more accurate information in regards to populating the final model.

In summary, my IHC experiments, along with collaboratory work that highlighted distributions of other proteins, represent a systemic analysis of the cell-wide distribution patterns of calcium signaling proteins belonging to the IP3-Ca^{2+} pathway in Purkinje cells (Haberl et al.,

in preparation). Across our IHC analysis, a wide range of both homogeneous and heterogeneous distribution patterns was observed, supporting our hypothesis that not all calcium signaling molecules are evenly distributed across the soma (Haberl et al., in preparation). Using electron tomography, we reconstructed a precise 3D ultrastructure of the intracellular space and were able to observe, quantify, and characterize the heterogeneous nature of the somatic ultrastructure (Fig. 1.2; Haberl et al., in preparation). This allowed us to quantify calcium diffusion rates that consider the varying orientation and distance of the ER relative to the PM, which we observed throughout our EM datasets. Even with idealized geometries, these calcium simulations reveal the somatic ultrastructure's potential to influence calcium signaling, both passively and actively, across the large "open space" of the soma (Haberl et al., in preparation). It was also revealed, using this idealized model, that varying IP3R and RyR density across the ER membrane dramatically alters calcium signaling (Haberl et al., in preparation). Once complete, it will enable future studies at an unprecedented level to explore how realistic membrane ultrastructure and accurate protein localization influence calcium handling within neuronal somas. Recent studies have already begun to characterize the ER's many contact points with other organelles and their potential functional roles in fine structural detail (Wu et al., 2017). In combination with our own research, we hope our final model will enable future studies to continue to further extrapolate the neuronal ultrastructure's functional role in modulating important cellular functions.

MATERIALS AND METHODS

Animals

All animal procedures were approved by the Institutional Animal Care and Use Committee (IACUC, protocol number S12254) of UC San Diego and followed all relevant ethical regulations regarding animal research. Wild-type C57BL/6J (Jackson Laboratories) male and female mice were used from postnatal days 45 to 50, for immunohistochemistry (IHC) experiments. For electron microscopy experiments, a single male C57BL/6NHsd mouse was used on postnatal day 40.

Tissue Preparation for Neuronal Imaging Experiments

To acquire tissue samples for IHC experiments, C57BL/6J mice were anesthetized with 90 µl of ketamine administered through intraperitoneal injection. Mice were then transcardially perfused at room temperature (37℃) and first flushed for 5 minutes with a 1x PBS, phosphate buffer saline, and heparin solution. The mice were then perfused for 15 minutes with a 4% paraformaldehyde (PFA) solution diluted from a 16% PFA stock solution (Electron Microscopy Sciences 15710) in 1X PBS. Immediately following the perfusion, the mice's whole brains were extracted and fixed in the remaining 4% PFA solution overnight at 4℃. Whole brains were then transferred into a 30% sucrose solution for a minimum of 48 hours at 4℃. Using a Leica microtome, freeze sectioning of the cerebellum was performed and 50 µm thick sagittal slices were collected and placed in cryo-preservative solution at -20℃ for a minimum of 24 hours. Tissue samples acquired for electron microscopy (EM) experiments were performed by Matthias Haberl at the NCMIR (National Center for Microscopy and Imaging Research) and followed the same procedures described in Haberl et al., 2018.

Immunohistochemistry (IHC)

Free floating cerebellar slices spanning the Vermis region of the Cerebellum were selected for immunohistochemistry experiments. Immunohistochemistry procedures were performed as described previously (Haberl et al., 2018). Chosen cerebellar tissue slices were first washed in ice cold 1X phosphate buffer saline (PBS) for ten minutes, three times. Tissue slices were then permeabilized for ten minutes at room temperature (37℃) in 1X PBS containing 1% Triton-X (diluted from 10% Triton-X solution [Sigma Aldrich 10789704001]). Permeabilized tissues were again washed in 1X PBS for ten minutes, three times. Tissue slices were then washed in a PBS based blocking buffer and incubated overnight at 4℃. Blocking buffer is comprised of 3% normal donkey serum (NDS) (Sigma Aldrich D9663), 1% bovine serum albumin (BSA), 1% cold water fish gelatin (diluted from 10% fish gelatin) and 0.1% Triton-X (Sigma Aldrich 10789704001).

Before primary antibody staining, if the primary antibody's protein receptor was raised in mouse, the tissue slices were further prepped to minimize background fluorescence. For certain experiments, tissue slices were incubated for an additional 2 hours at room temperature (37℃) in a Mouse-on-Mouse staining solution containing 0.1mg/mL anti mouse IgG (H+L) polyclonal antibody (Jackson 2338476). After the two-hour period, the tissue slices were washed three times in working buffer for ten minutes each time.

Slices were washed with an ice cold working buffer three times for ten minutes at 4℃. This working buffer consists of 10% blocking buffer, 0.1% Triton-X (Sigma Aldrich 10789704001), and 1X PBS. Primary antibody staining was performed by incubating tissue slices for 72 hours at 4℃ in working buffer solution containing primary antibodies. List of

primary antibodies used: 1/800 guinea Pig anti Calbindin polyclonal (Synaptic Systems 214004), 1/250 Rabbit anti PMCA2 polyclonal (abcam ab3529) 1/100 Rabbit anti CKAP4/ CLIMP63 polyclonal (Proteintech 16686-1-AP), 0.1mg/mL anti Mouse IgG (H+L) polyclonal (Jackson 2338476), 1/100 Rabbit anti IP3R1 polyclonal (Invitrogen PA1-901), 1/100 Rabbit anti RTN4 polyclonal (Proteintech 10950-1-AP), 1/100 Mouse anti RyR1 monoclonal (Invitrogen MA3-925), 1/100 Rabbit anti SERCA2 polyclonal (Novus NB100-237)), 1/100 Rabbit anti TOM20 polyclonal (Proteintech 11802-1-AP).

Primary antibody tissue slices after the 72-hour period were removed from the primary antibody solution and washed three times in ice cold working buffer solution for five minutes. Secondary antibody staining was performed by incubating tissue slices for 24 hours at 4℃ in working buffer solution containing secondary antibodies (working buffer is made the same as described previously). Secondary antibodies were conjugated to Alexa 488, 594, and 647 fluorophores. All secondary antibodies were raised in donkeys. After the 24-hour secondary antibody solution incubation process, tissue slices were washed with ice cold 1X PBS for 5 minutes, three times. Tissue slices were then stained and mounted on a microscope slide using DAPI (4′,6-diamidino-2-phenylindole) Fluoromount-G mounting media (SouthernBiotech 0100-20) in order to stain the nuclei of the Purkinje cells. The slides were then sealed with glass coverslips.

Confocal Microscopy and Analysis

Stained cerebellar tissue slices (described above) were acquired and imaged in order to obtain volumetric confocal image datasets of Purkinje cells located within the Vermis region on lobes IV/V and VI. Images were taken at the Nikon Imaging Center at UC San Diego with the

Nikon A1 Confocal and deconvolved with the Landweber algorithm by NIS-Elements Software. For each target protein, 18 neurons were imaged, selected, and analyzed across three different brains. The only exception to this is SERCA2, in which only 5 neurons were imaged, selected, and analyzed across two brains. For each neuron 11-21 sequential z-step images emanating from the center of the neuron were selected and analyzed. The center of the neuron was estimated by measuring and comparing the maximal somatic and nuclear widths. Once selected, contour masks based on calbindin staining were generated to outline the plasma membrane boundary of the Purkinje neurons, while DAPI staining was used to generate Purkinje nuclei contour masks (Fig. 2.1a-e). These contour masks were automatically generated using IMOD software and were hand corrected for each neuron across its z-step range. Purkinje soma and dendrite boundary cut-off points were determined by utilizing the progression of cellular curvature to estimate the natural inflection points between the larger somatic space and smaller diameter of the dendritic opening. Finalized contour masks were used to isolate fluorescence within the somatic space, which was then analyzed utilizing Matlab scripts created by Evan Campbell. Background fluorescence of target proteins was estimated for each z step image of each neuron in one of two ways: by measuring the averaged fluorescence (1) within the Purkinje cell nuclei or (2) drawing the background ROI of a granule neuron nuclei near the target Purkinje cell. Target protein fluorescence was extracted between the soma boundary mask and the nucleus boundary. Background fluorescence was subtracted from the target protein fluorescence and measured across the target cell population (n=18) using both angular and radial analysis techniques. A standard coordinate system was used for every cell, so that the fluorescence could be analyzed along standardized angular and radial axes to measure its averaged abundance across the cell population (Fig. 2.1-2.5). The standard coordinate system rotates every image, so the apical

dendrite (dendritic pole) is at 270°, the axonal pole is at 90°, and the nucleus centroid is located at the origin (0,0) and aligned linearly with the apical dendrite (Fig. 2.1b). Angular fluorescence intensity was analyzed by imposing the coordinate system, described above, onto each cell and segmenting the cytoplasmic space into twelve 30° bins (Fig. 2.1g). In each 30° bin and across each cell the fluorescence intensity was averaged across 0°-360° for the entire cell population, allowing the angular fluorescence distribution for each protein target to be calculated. Radial fluorescence intensity was analyzed by normalizing the radial vector lengths emanating laterally from the nuclear boundary to the soma boundary, across 0°-360° and within each 30° bin (Fig. 2.1h). The normalized radii vectors were scaled and averaged across the cell population for each protein target across 0°-360° and within each 30° bin. Radial fluorescence distribution patterns were calculated across the cell population using the average normalized and scaled radii vectors for each protein target (Fig. 2.1h). Calculations for both angular and radial analysis techniques were performed using One-way ANOVAS significance tests in Prism GraphPad.

Electron Microscopy Techniques and 3D Ultrastructure Reconstruction

Volumetric image datasets of the axonal and dendritic pole regions of mouse cerebellar Purkinje neurons were acquired using electron tomography (ET). One large-scale volumetric image dataset of a cerebellar Purkinje soma was acquired using Serial block-face scanning electron microscopy (SBEM) (Haberl et al., 2018). Methods for both SBEM and ET experiments were performed as described in Haberl et al. 2018. ET volumetric datasets were acquired at 2.1-3 nm voxelsize and reconstructed at 4.2-6 nm voxelsize in x/y/z. Imaging dimensions for the Tomo 2 dataset shown in Figure 1.2 are as follows: Tomo2: reconstructed voxelsize in x/y/z 6 nm; Image volume dimensions: 12 x 12 x 2.62 μm^3.

CDeep3M, an open source deep-learning image segmentation algorithm, was used to generate the initial segmentations of the Purkinje soma's subcellular ultrastructure (Haberl et al., 2018). The plasma membrane, nucleus, Golgi apparatus, mitochondria, and endoplasmic reticulum were reconstructed across five ET volumetric image datasets. Manual hand annotations and subsequent smaller EM training datasets were performed using IMOD software to increase the accuracy and precision of CDeep3M's segmentation predictions. Manual corrections and continual training of CDeep3M was conducted to produce the finalized 3D models of the somatic ultrastructure.

Purkinje Soma Calcium Diffusion Model

The calcium diffusion model, using partial differential equations, was created by Justin Laughlin at the Rangamani Lab, UC San Diego. The model has been constructed to simulate realistic spatiotemporal calcium dynamics in Purkinje somas, by incorporating the structural and spatial information obtained from the experiments described above.

Acknowledgment

Materials produced and used in this paper are co-authored with Haberl, Matthias G; Laughlin, Justin; Campbell, Evan P; Robinson, Kaitlyn; Wang, Yuning; Makrakis, Lukas; Nguyen, Andrew; Oshiro, Justin; Phan, Sebastien, Bushong, Eric; Deerinck, Thomas D; Ellisman, Mark H; Rangamani, Padmini; Bloodgood, Brenda L. Work from this thesis in part is currently being prepared for submission for publication of the material. Matthias Haberl is the primary investigator of this project. Lukas Makrakis is the author of this thesis and is a co-author of this material.

REFERENCES

Allbritton, N. L., Meyer, T., & Stryer, L. (1992). Range of messenger action of calcium ion and inositol 1,4,5-trisphosphate. *Science (New York, N.Y.)*, *258*(5089), 1812–1815. https://doi.org/10.1126/science.1465619

Baba-Aissa, F., Raeymaekers, L., Wuytack, F., De Greef, C., Missiaen, L., & Casteels, R. (1996). Distribution of the organellar Ca2+ transport ATPase SERCA2 isoforms in the cat brain. *Brain research*, *743*(1-2), 141–153. https://doi.org/10.1016/s0006-8993(96)01037-2

Banno, T., & Kohno, K. (1998). Conformational changes of the smooth endoplasmic reticulum are facilitated by L-glutamate and its receptors in rat Purkinje cells. *The Journal of comparative neurology*, *402*(2), 252–263.

Berridge M. J. (1993). Inositol trisphosphate and calcium signalling. *Nature*, *361*(6410), 315–325. https://doi.org/10.1038/361315a0

Berridge M. J. (1998). Neuronal calcium signaling. *Neuron*, *21*(1), 13–26. https://doi.org/10.1016/s0896-6273(00)80510-3

Berridge M. J. (2016). The Inositol Trisphosphate/Calcium Signaling Pathway in Health and Disease. *Physiological reviews*, *96*(4), 1261–1296. https://doi.org/10.1152/physrev.00006.2016

Berridge, M. J., Bootman, M. D., & Roderick, H. L. (2003). Calcium signalling: dynamics, homeostasis and remodelling. *Nature reviews. Molecular cell biology*, *4*(7), 517–529. https://doi.org/10.1038/nrm1155

Berridge, M. J., Lipp, P., & Bootman, M. D. (2000). The versatility and universality of calcium signalling. *Nature reviews. Molecular cell biology*, *1*(1), 11–21. https://doi.org/10.1038/35036035

Biwer, L. A., & Isakson, B. E. (2017). Endoplasmic reticulum-mediated signalling in cellular microdomains. *Acta physiologica (Oxford, England)*, *219*(1), 162–175. https://doi.org/10.1111/apha.12675

Bloodgood, B. L., & Sabatini, B. L. (2007). Ca(2+) signaling in dendritic spines. *Current opinion in neurobiology*, *17*(3), 345–351. https://doi.org/10.1016/j.conb.2007.04.003

Brini, M., Calì, T., Ottolini, D., & Carafoli, E. (2014). Neuronal calcium signaling: function and dysfunction. *Cellular and molecular life sciences : CMLS*, *71*(15), 2787–2814. https://doi.org/10.1007/s00018-013-1550-7

Britzolaki, A., Saurine, J., Flaherty, E., Thelen, C., & Pitychoutis, P. M. (2018). The SERCA2: A Gatekeeper of Neuronal Calcium Homeostasis in the Brain. *Cellular and molecular neurobiology*, *38*(5), 981–994. https://doi.org/10.1007/s10571-018-0583-8

Brown, S. A., & Loew, L. M. (2012). Computational analysis of calcium signaling and membrane electrophysiology in cerebellar Purkinje neurons associated with ataxia. *BMC systems biology*, *6*, 70. https://doi.org/10.1186/1752-0509-6-70

Brown, S. A., Morgan, F., Watras, J., & Loew, L. M. (2008). Analysis of phosphatidylinositol-4,5-bisphosphate signaling in cerebellar Purkinje spines. *Biophysical journal*, *95*(4), 1795–1812. https://doi.org/10.1529/biophysj.108.130195

Chang, C. L., Chen, Y. J., & Liou, J. (2017). ER-plasma membrane junctions: Why and how do we study them?. *Biochimica et biophysica acta. Molecular cell research*, *1864*(9), 1494–1506. https://doi.org/10.1016/j.bbamcr.2017.05.018

Chen-Engerer, H. J., Hartmann, J., Karl, R. M., Yang, J., Feske, S., & Konnerth, A. (2019). Two types of functionally distinct Ca^{2+} stores in hippocampal neurons. *Nature communications*, *10*(1), 3223. https://doi.org/10.1038/s41467-019-11207-8

Chung, W. Y., Jha, A., Ahuja, M., & Muallem, S. (2017). Ca^{2+} influx at the ER/PM junctions. *Cell calcium*, *63*, 29–32. https://doi.org/10.1016/j.ceca.2017.02.009

Cooling, M., Hunter, P., & Crampin, E. J. (2007). Modeling hypertrophic IP3 transients in the cardiac myocyte. *Biophysical journal*, *93*(10), 3421–3433. https://doi.org/10.1529/biophysj.107.110031

Doi, T., Kuroda, S., Michikawa, T., & Kawato, M. (2005). Inositol 1,4,5-trisphosphate-dependent Ca2+ threshold dynamics detect spike timing in cerebellar Purkinje cells. *The Journal of neuroscience : the official journal of the Society for Neuroscience*, *25*(4), 950–961. https://doi.org/10.1523/JNEUROSCI.2727-04.2005

Eilers, J., Callewaert, G., Armstrong, C., & Konnerth, A. (1995). Calcium signaling in a narrow somatic submembrane shell during synaptic activity in cerebellar Purkinje neurons. *Proceedings of the National Academy of Sciences of the United States of America*, *92*(22), 10272–10276. https://doi.org/10.1073/pnas.92.22.10272

Ellisman, M. H., Deerinck, T. J., Ouyang, Y., Beck, C. F., Tanksley, S. J., Walton, P. D., Airey, J. A., & Sutko, J. L. (1990). Identification and localization of ryanodine binding proteins in the avian central nervous system. *Neuron*, *5*(2), 135–146. https://doi.org/10.1016/0896-6273(90)90304-x

Empson, R. M., Garside, M. L., & Knöpfel, T. (2007). Plasma membrane Ca2+ ATPase 2 contributes to short-term synapse plasticity at the parallel fiber to Purkinje neuron synapse. *The Journal of neuroscience : the official journal of the Society for Neuroscience*, *27*(14), 3753–3758. https://doi.org/10.1523/JNEUROSCI.0069-07.2007

Empson, R. M., & Knöpfel, T. (2012). Functional integration of calcium regulatory mechanisms at Purkinje neuron synapses. *Cerebellum (London, England)*, *11*(3), 640–650. https://doi.org/10.1007/s12311-010-0185-6

Fierro, L., & Llano, I. (1996). High endogenous calcium buffering in Purkinje cells from rat cerebellar slices. *The Journal of physiology*, *496 (Pt 3)*(Pt 3), 617–625. https://doi.org/10.1113/jphysiol.1996.sp021713

Fierro, L., DiPolo, R., & Llano, I. (1998). Intracellular calcium clearance in Purkinje cell somata from rat cerebellar slices. *The Journal of physiology*, *510 (Pt 2)*(Pt 2), 499–512. https://doi.org/10.1111/j.1469-7793.1998.499bk.x

Fink, C. C., Slepchenko, B., Moraru, I. I., Watras, J., Schaff, J. C., & Loew, L. M. (2000). An image-based model of calcium waves in differentiated neuroblastoma cells. *Biophysical journal*, *79*(1), 163–183. https://doi.org/10.1016/S0006-3495(00)76281-3

Gambarotto, D., Zwettler, F. U., Le Guennec, M., Schmidt-Cernohorska, M., Fortun, D., Borgers, S., Heine, J., Schloetel, J. G., Reuss, M., Unser, M., Boyden, E. S., Sauer, M., Hamel, V., & Guichard, P. (2019). Imaging cellular ultrastructures using expansion microscopy (U-ExM). *Nature methods*, *16*(1), 71–74. https://doi.org/10.1038/s41592-018-0238-1

Gao, G., Zhu, C., Liu, E., & Nabi, I. R. (2019). Reticulon and CLIMP-63 regulate nanodomain organization of peripheral ER tubules. *PLoS biology*, *17*(8), e3000355. https://doi.org/10.1371/journal.pbio.3000355

Ghosh, A., & Greenberg, M. E. (1995). Calcium signaling in neurons: molecular mechanisms and cellular consequences. *Science (New York, N.Y.)*, *268*(5208), 239–247. https://doi.org/10.1126/science.7716515

Goto, J., & Mikoshiba, K. (2011). Inositol 1,4,5-trisphosphate receptor-mediated calcium release in Purkinje cells: from molecular mechanism to behavior. *Cerebellum (London, England)*, *10*(4), 820–833. https://doi.org/10.1007/s12311-011-0270-5

Goyal, U., & Blackstone, C. (2013). Untangling the web: mechanisms underlying ER network formation. *Biochimica et biophysica acta*, *1833*(11), 2492–2498. https://doi.org/10.1016/j.bbamcr.2013.04.009

Grienberger, C., & Konnerth, A. (2012). Imaging calcium in neurons. *Neuron*, *73*(5), 862–885. https://doi.org/10.1016/j.neuron.2012.02.011

Gruol, D. L., Netzeband, J. G., & Nelson, T. E. (2010). Somatic Ca2+ signaling in cerebellar Purkinje neurons. *Journal of neuroscience research*, *88*(2), 275–289. https://doi.org/10.1002/jnr.22204

Gruol, D., Manto, M., & Haines, D. (2012). Ca2+ signaling in cerebellar Purkinje neurons--editorial. *Cerebellum (London, England)*, *11*(3), 605–608. https://doi.org/10.1007/s12311-012-0404-4

Haberl, M. G., Churas, C., Tindall, L., Boassa, D., Phan, S., Bushong, E. A., Madany, M., Akay, R., Deerinck, T. J., Peltier, S. T., & Ellisman, M. H. (2018). CDeep3M — Plug-and-Play

cloud-based deep learning for image segmentation. *Nature Methods*, 15, 677–680. https://doi.org/10.1038/s41592-018-0106-z

Hartmann, J., Dragicevic, E., Adelsberger, H., Henning, H. A., Sumser, M., Abramowitz, J., Blum, R., Dietrich, A., Freichel, M., Flockerzi, V., Birnbaumer, L., & Konnerth, A. (2008). TRPC3 channels are required for synaptic transmission and motor coordination. *Neuron*, *59*(3), 392–398. https://doi.org/10.1016/j.neuron.2008.06.009

Hartmann, J., Karl, R. M., Alexander, R. P., Adelsberger, H., Brill, M. S., Rühlmann, C., Ansel, A., Sakimura, K., Baba, Y., Kurosaki, T., Misgeld, T., & Konnerth, A. (2014). STIM1 controls neuronal Ca^{2+} signaling, mGluR1-dependent synaptic transmission, and cerebellar motor behavior. *Neuron*, *82*(3), 635–644. https://doi.org/10.1016/j.neuron.2014.03.027

Higley, M. J., & Sabatini, B. L. (2008). Calcium signaling in dendrites and spines: practical and functional considerations. *Neuron*, *59*(6), 902–913. https://doi.org/10.1016/j.neuron.2008.08.020

Hirano T. (2018). Purkinje Neurons: Development, Morphology, and Function. *Cerebellum (London, England)*, *17*(6), 699–700. https://doi.org/10.1007/s12311-018-0985-7

Hernjak, N., Slepchenko, B. M., Fernald, K., Fink, C. C., Fortin, D., Moraru, I. I., Watras, J., & Loew, L. M. (2005). Modeling and analysis of calcium signaling events leading to long-term depression in cerebellar Purkinje cells. *Biophysical journal*, *89*(6), 3790–3806. https://doi.org/10.1529/biophysj.105.065771

Kano, M., Garaschuk, O., Verkhratsky, A., & Konnerth, A. (1995). Ryanodine receptor-mediated intracellular calcium release in rat cerebellar Purkinje neurones. *The Journal of physiology*, *487*(1), 1–16. https://doi.org/10.1113/jphysiol.1995.sp020857

Kraft R. (2015). STIM and ORAI proteins in the nervous system. *Channels (Austin, Tex.)*, *9*(5), 245–252. https://doi.org/10.1080/19336950.2015.1071747

Kurnellas, M. P., Lee, A. K., Li, H., Deng, L., Ehrlich, D. J., & Elkabes, S. (2007). Molecular alterations in the cerebellum of the plasma membrane calcium ATPase 2 (PMCA2)-null mouse indicate abnormalities in Purkinje neurons. *Molecular and cellular neurosciences*, *34*(2), 178–188. https://doi.org/10.1016/j.mcn.2006.10.010

Kuwajima, G., Futatsugi, A., Niinobe, M., Nakanishi, S., & Mikoshiba, K. (1992). Two types of ryanodine receptors in mouse brain: skeletal muscle type exclusively in Purkinje cells and cardiac muscle type in various neurons. *Neuron*, *9*(6), 1133–1142. https://doi.org/10.1016/0896-6273(92)90071-k

Llano, I., DiPolo, R., & Marty, A. (1994). Calcium-induced calcium release in cerebellar Purkinje cells. *Neuron*, *12*(3), 663–673. https://doi.org/10.1016/0896-6273(94)90221-6

Martone, M. E., Zhang, Y., Simpliciano, V. M., Carragher, B. O., & Ellisman, M. H. (1993). Three-dimensional visualization of the smooth endoplasmic reticulum in Purkinje cell

dendrites. *The Journal of neuroscience : the official journal of the Society for Neuroscience*, *13*(11), 4636–4646. https://doi.org/10.1523/JNEUROSCI.13-11-04636.1993

Maskey, D., Pradhan, J., Kim, H. J., Park, K. S., Ahn, S. C., & Kim, M. J. (2010). Immunohistochemical localization of calbindin D28-k, parvalbumin, and calretinin in the cerebellar cortex of the circling mouse. *Neuroscience letters*, *483*(2), 132–136. https://doi.org/10.1016/j.neulet.2010.07.077

Neher, E., & Augustine, G. J. (1992). Calcium gradients and buffers in bovine chromaffin cells. *The Journal of physiology*, *450*, 273–301. https://doi.org/10.1113/jphysiol.1992.sp019127

Nimchinsky, E. A., Sabatini, B. L., & Svoboda, K. (2002). Structure and function of dendritic spines. *Annual review of physiology*, *64*, 313–353. https://doi.org/10.1146/annurev.physiol.64.081501.160008

Niswender, C. M., & Conn, P. J. (2010). Metabotropic glutamate receptors: physiology, pharmacology, and disease. *Annual review of pharmacology and toxicology*, *50*, 295–322. https://doi.org/10.1146/annurev.pharmtox.011008.145533

Nixon-Abell, J., Obara, C. J., Weigel, A. V., Li, D., Legant, W. R., Xu, C. S., Pasolli, H. A., Harvey, K., Hess, H. F., Betzig, E., Blackstone, C., & Lippincott-Schwartz, J. (2016). Increased spatiotemporal resolution reveals highly dynamic dense tubular matrices in the peripheral ER. *Science (New York, N.Y.)*, *354*(6311), aaf3928. https://doi.org/10.1126/science.aaf3928

Orrenius, S., Zhivotovsky, B., & Nicotera, P. (2003). Regulation of cell death: the calcium-apoptosis link. *Nature reviews. Molecular cell biology*, *4*(7), 552–565. https://doi.org/10.1038/nrm1150

Park, S. H., & Blackstone, C. (2010). Further assembly required: construction and dynamics of the endoplasmic reticulum network. *EMBO reports*, *11*(7), 515–521. https://doi.org/10.1038/embor.2010.92

Renvoisé, B., & Blackstone, C. (2010). Emerging themes of ER organization in the development and maintenance of axons. *Current opinion in neurobiology*, *20*(5), 531–537. https://doi.org/10.1016/j.conb.2010.07.001

Ross W. N. (2012). Understanding calcium waves and sparks in central neurons. *Nature reviews. Neuroscience*, *13*(3), 157–168. https://doi.org/10.1038/nrn3168

Schroeder, L. K., Barentine, A., Merta, H., Schweighofer, S., Zhang, Y., Baddeley, D., Bewersdorf, J., & Bahmanyar, S. (2019). Dynamic nanoscale morphology of the ER surveyed by STED microscopy. *The Journal of cell biology*, *218*(1), 83–96. https://doi.org/10.1083/jcb.201809107

Sepúlveda, M. R., Hidalgo-Sánchez, M., & Mata, A. M. (2004). Localization of endoplasmic reticulum and plasma membrane Ca2+-ATPases in subcellular fractions and sections of pig cerebellum. *The European journal of neuroscience*, *19*(3), 542–551. https://doi.org/10.1111/j.0953-816x.2003.03156.x

Sepúlveda, M. R., Hidalgo-Sánchez, M., Marcos, D., & Mata, A. M. (2007). Developmental distribution of plasma membrane Ca2+-ATPase isoforms in chick cerebellum. *Developmental dynamics : an official publication of the American Association of Anatomists*, *236*(5), 1227–1236. https://doi.org/10.1002/dvdy.21131

Sharp, A. H., Nucifora, F. C., Jr, Blondel, O., Sheppard, C. A., Zhang, C., Snyder, S. H., Russell, J. T., Ryugo, D. K., & Ross, C. A. (1999). Differential cellular expression of isoforms of inositol 1,4,5-triphosphate receptors in neurons and glia in brain. *The Journal of comparative neurology*, *406*(2), 207–220.

Sherkhane, P., & Kapfhammer, J. P. (2013). The plasma membrane Ca2+-ATPase2 (PMCA2) is involved in the regulation of Purkinje cell dendritic growth in cerebellar organotypic slice cultures. *Neural plasticity*, *2013*, 321685. https://doi.org/10.1155/2013/321685

Shibata, Y., Shemesh, T., Prinz, W. A., Palazzo, A. F., Kozlov, M. M., & Rapoport, T. A. (2010). Mechanisms determining the morphology of the peripheral ER. *Cell*, *143*(5), 774–788. https://doi.org/10.1016/j.cell.2010.11.007

Stefan, C. J., Manford, A. G., & Emr, S. D. (2013). ER-PM connections: sites of information transfer and inter-organelle communication. *Current opinion in cell biology*, *25*(4), 434–442. https://doi.org/10.1016/j.ceb.2013.02.020

Subedi, K. P., Ong, H. L., & Ambudkar, I. S. (2017). Assembly of ER-PM Junctions: A Critical Determinant in the Regulation of SOCE and TRPC1. *Advances in experimental medicine and biology*, *981*, 253–276. https://doi.org/10.1007/978-3-319-55858-5_11

Sugawara, T., Hisatsune, C., Le, T. D., Hashikawa, T., Hirono, M., Hattori, M., Nagao, S., & Mikoshiba, K. (2013). Type 1 inositol trisphosphate receptor regulates cerebellar circuits by maintaining the spine morphology of purkinje cells in adult mice. *The Journal of neuroscience : the official journal of the Society for Neuroscience*, *33*(30), 12186–12196. https://doi.org/10.1523/JNEUROSCI.0545-13.2013

Terasaki, M., Slater, N. T., Fein, A., Schmidek, A., & Reese, T. S. (1994). Continuous network of endoplasmic reticulum in cerebellar Purkinje neurons. *Proceedings of the National Academy of Sciences of the United States of America*, *91*(16), 7510–7514. doi:10.1073/pnas.91.16.7510

Thillaiappan, N. B., Chavda, A. P., Tovey, S. C., Prole, D. L., & Taylor, C. W. (2017). Ca^{2+} signals initiate at immobile IP_3 receptors adjacent to ER-plasma membrane junctions. *Nature communications*, *8*(1), 1505. https://doi.org/10.1038/s41467-017-01644-8

Tillberg, P. W., Chen, F., Piatkevich, K. D., Zhao, Y., Yu, C. C., English, B. P., Gao, L., Martorell, A., Suk, H. J., Yoshida, F., DeGennaro, E. M., Roossien, D. H., Gong, G., Seneviratne, U., Tannenbaum, S. R., Desimone, R., Cai, D., & Boyden, E. S. (2016). Protein-retention expansion microscopy of cells and tissues labeled using standard fluorescent proteins and antibodies. *Nature biotechnology*, *34*(9), 987–992. https://doi.org/10.1038/nbt.3625

Voeltz, G. K., Rolls, M. M., & Rapoport, T. A. (2002). Structural organization of the endoplasmic reticulum. *EMBO reports*, *3*(10), 944–950. https://doi.org/10.1093/embo-reports/kvf202

Walton, P. D., Airey, J. A., Sutko, J. L., Beck, C. F., Mignery, G. A., Südhof, T. C., Deerinck, T. J., & Ellisman, M. H. (1991). Ryanodine and inositol trisphosphate receptors coexist in avian cerebellar Purkinje neurons. *The Journal of cell biology*, *113*(5), 1145–1157. https://doi.org/10.1083/jcb.113.5.1145

Wassie, A. T., Zhao, Y., & Boyden, E. S. (2019). Expansion microscopy: principles and uses in biological research. *Nature methods*, *16*(1), 33–41. https://doi.org/10.1038/s41592-018-0219-4

West, A. E., Chen, W. G., Dalva, M. B., Dolmetsch, R. E., Kornhauser, J. M., Shaywitz, A. J., Takasu, M. A., Tao, X., & Greenberg, M. E. (2001). Calcium regulation of neuronal gene expression. *Proceedings of the National Academy of Sciences of the United States of America*, *98*(20), 11024–11031. https://doi.org/10.1073/pnas.191352298

Wu, Y., Whiteus, C., Xu, C. S., Hayworth, K. J., Weinberg, R. J., Hess, H. F., & De Camilli, P. (2017). Contacts between the endoplasmic reticulum and other membranes in neurons. *Proceedings of the National Academy of Sciences of the United States of America*, *114*(24), E4859–E4867. https://doi.org/10.1073/pnas.1701078114

Yang, Y. S., & Strittmatter, S. M. (2007). The reticulons: a family of proteins with diverse functions. *Genome biology*, *8*(12), 234. https://doi.org/10.1186/gb-2007-8-12-234

Zhang, H., & Hu, J. (2016). Shaping the Endoplasmic Reticulum into a Social Network. *Trends in cell biology*, *26*(12), 934–943. https://doi.org/10.1016/j.tcb.2016.06.002